Agreement No. NAG3-1432 **Final Report**

Graphite Fiber Textile Preform/Cooper Matrix Composites

IN-24
31055

by
George J. Filatovs

of
Department of Mechanical Engineering
North Carolina A & T State University
1601 E. Market St., Greensboro, NC 27411

A Final Summary Report

Submitted to
Dr. R. V. Miner (5120)
Technical Monitor
NASA Lewis Research Center
Advanced Metallics Branch
Cleveland, OH

August 24, 1998

ABSTRACT

The purpose of this research was to produce a finned tube constructed of a highly conductive braided graphite fiber preform infiltrated with a copper matrix. In addition, the tube was to be fabricated with an integral geometry. The preform was integral in the sense that the tube and the fin could be braided to yield one continuous part. This composite component is a candidate for situations with high heat transmitting and radiation requirements. A proof-of-concept finned tube was braided and infiltrated with a copper matrix proving that a viable process was developed to fabricate the desired component.

Braiding of high conductivity carbon fibers required much trial-and-error and development of special procedures. There are many tradeoffs between braidability and fiber conductivity. To understand the properties and structure of the braided finned tube, an geometric model of the braid structure was derived. This derivation set the basis for the research because knowing the tow orientations helped decipher the thermal as well as the mechanical and conduction tendencies. Infiltration of the fibers into a copper matrix was a complex procedure, and was performed by TRA, of Salt Lake City, Utah, using a proprietary process. Several batches were fabricated with a final, high quality batch serving as a confirming proof-of-concept.

ABSTRACT

The purpose of this research was to produce a finned tube constructed of a highly conductive braided graphite fiber preform infiltrated with a copper matrix. In addition, the tube was to be fabricated with an integral geometry. The preform was integral in the sense that the tube and the fin could be braided to yield one continuous part. This composite component is a candidate for situations with high heat transmitting and radiation requirements. A proof-of-concept finned tube was braided and infiltrated with a copper matrix proving that a viable process was developed to fabricate the desired component.

Braiding of high conductivity carbon fibers required much trial-and-error and development of special procedures. There are many tradeoffs between braidability and fiber conductivity. To understand the properties and structure of the braided finned tube, an geometric model of the braid structure was derived. This derivation set the basis for the research because knowing the tow orientations helped decipher the thermal as well as the mechanical and conduction tendencies. Infiltration of the fibers into a copper matrix was a complex procedure, and was performed by TRA, of Salt Lake City, Utah, using a proprietary process. Several batches were fabricated with a final, high quality batch serving as a confirming proof-of-concept.

Acknowledgments

This research was supported by NASA Lewis Research Center, Cleveland, OH, through grant No. NASA NAG3-1432. The authors are grateful for this support, and the technical advice and assistance of the NASA grant monitor, Dr. Robert V. Miner. We would also particularly like to thank Dr. David Ellis for his assistance. The braiding was accomplished with much help from Rona Reid of NC State University. Portions of the work on which this report is based formed part of the thesis requirements for the degree of Master of Science for the first author.

TABLE OF CONTENTS

LIST OF FIGURES

LIST OF TABLES

CHAPTER ONE

Introduction to Research

1.1 High Conductivity Material System

This research initiated because of the need for components with good heat transmitting characteristics as well as structural integrity at high temperatures. Copper, a candidate material because of its great thermal conduction, can not be used unreinforced because at high temperatures copper creeps. Graphite fibers with conductivities exceeding that of copper are available. As the fibers degree of graphitization increases, its thermal conductivity and strength increase in direct proportions. Therefore, high conductivity graphite was chosen to reinforce the copper because it could offer structural strength and high heat conduction properties at high temperatures. Copper and graphite form a fibrous metal matrix composite (MMC) which in this case means copper is the binding material and the graphite preform is infiltrated with copper (Jones 2,4).

Advantages that can be expected in using a copper/graphite MMC as opposed to oxygen-free high conductivity (OFHC) copper or a graphite/epoxy composite are an increase in robustness at higher temperatures, a higher strength to weight ratio, a superior thermally conductive matrix, and an increase in overall thermal conduction. The target fibers of this research were K-1100 X fibers. Table 1.1 shows how copper and the K-1100 X fibers compare. Notice that the K-1100 X fibers offer a thermal conductivity

Table 1.1 Comparison of OFHC Copper and High Conductivity Graphite

Material	Tensile Strength	Elastic Modulus	Thermal Conductivity
Copper	0.03 Msi	16 Msi	223 Btu/Hr ft F ^{o}
K-1100 X Fibers	0.43	145	>1000

four and one-half times that of copper while providing extremely high values for the operating temperature and mechanical strength. Analysis of this table reveals that a more rigid, highly conductive, light structure would contain a majority of K-1100 X graphite fibers. Conversely, in order to make a tougher, heavier composite, more copper should be used. The relationship between the amount of fibers, and total volume in the a MMC is known as the fiber volume or volume fraction shown as:

$\left(\frac{\text{Volume}_{\text{fibers}}}{\text{Total Volume}_{\text{component}}}\right)$, or $\left(\frac{\text{Volume}_{\text{matrix}}}{\text{Total Volume}_{\text{component}}}\right)$. This knowledge is useful because in situations where thermal conduction is desired, more K-1100 X fibers should be used and in situations where bending or ductility is prominent, more copper should be used. In short, by controlling the volume fraction of the MMC, the mechanical properties of that component can be predicted.

Although copper/graphite MMCs offer several advantages, there are some problems that had to be overcome. These problems will be discussed in detail in chapter three.

1. 2 Integral Finned Geometry

When a high modulus MMC is machined the strength of the specimen will be lowered because fiber breakage will be introduced throughout the component. These high stress areas eventually cause failure of the composite. Additionally, the joining of components is a problem because joints are potential weak spots in the material that may fail when a load is applied around the high stress concentrations at the joints. A three dimensional (3-D) braid can produce integral components or shapes that are continuous without joints which retain their structural integrity eliminating the need for machining.

As a proof of the concept that complex integral braided shapes can be braided into near net shape, a finned tube was chosen.

Additional advantages of a 3-D finned tube are the increase in heat transfer rate as a result of the fins, the increase of structure rigidity because of the braid architecture, and the variety of finned shapes that can be fabricated. Figure 1.1 shows stiffness vs. thermal conduction tendencies of different fiber orientations. In order to get the maximum stiffness, the fibers must be aligned in the longitudinal direction; where as, transverse alignment allows the maximum heat transfer through the fins to occur. The final figure implies that the orientations of the fibers can be combined to give the desired properties in the directions along the fibers tows. In other words, specific orientations can be configured in order to absorb loads or project heat at and through specified locations. The ability to be able to control the orientations of these properties for individual needs is in the strength of the 3-D braid technology.

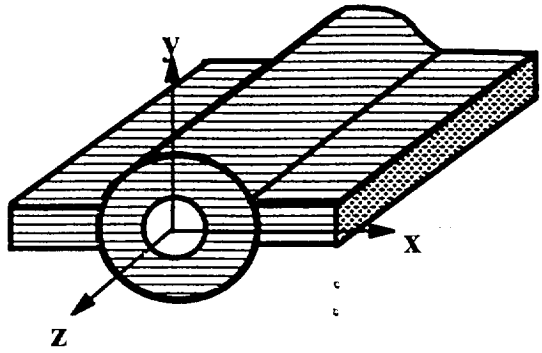

a) Maximum heat transfer

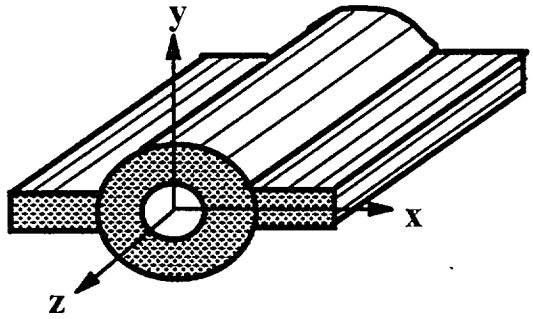

b) Maximum stiffness

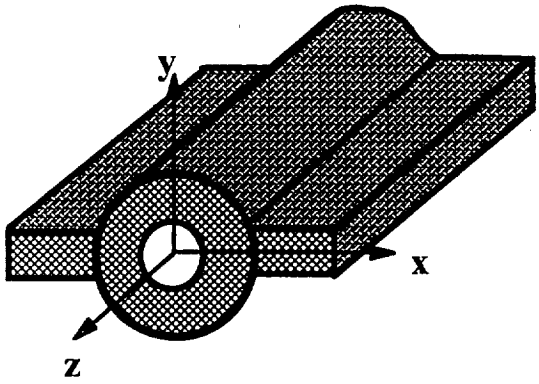

c) 3-D braid- a combination of a and b

Figure 1.1 - Mechanical Properties vs. Thermal Properties.
Note: z is braiding axis.

CHAPTER TWO

Braiding and Characterization of Preform

2.1 Braidability

Braidability, a term developed in this research, describes the collection of mechanical properties and materials phenomena that determine whether or not braiding a material is possible. Figures 2.1 - 2.6 summarize the manual braiding process. The first photo is of an empty carrier of the braiding machine. The next photo is a carrier being setup by taping the fiber tows to the green yarns and tying the green yarns to the elastic bands tied to the carrier. Figure 2.3 shows the different components used by the braiding machine. The last photos are of the fully setup carrier and the finished P100 HTS finned tube preform. Table 2.1 shows all of the materials that have been considered in this research. This table represents a considerable amount of work because in order to find the optimum material, each material had to be analyzed and tested as a function of more than one property. The results of these tests and analysis of the braiding process are shown in column four of table 2.1 as the braidability. Manual braiding is a complex skilled process and for this reason the braidability can not be determined by the factors in table 2.1 alone. Other factors that effect the braidability of a material are fiber breakage, inter-tow friction, and the process of beating up.

Fiber breakage is a significant problem with braiding high modulus materials. Figure 2.7 shows the stiffness vs. toughness trends for graphite fibers. From these trends, it can be seen that toughness is clearly the amount of energy that a material absorbs

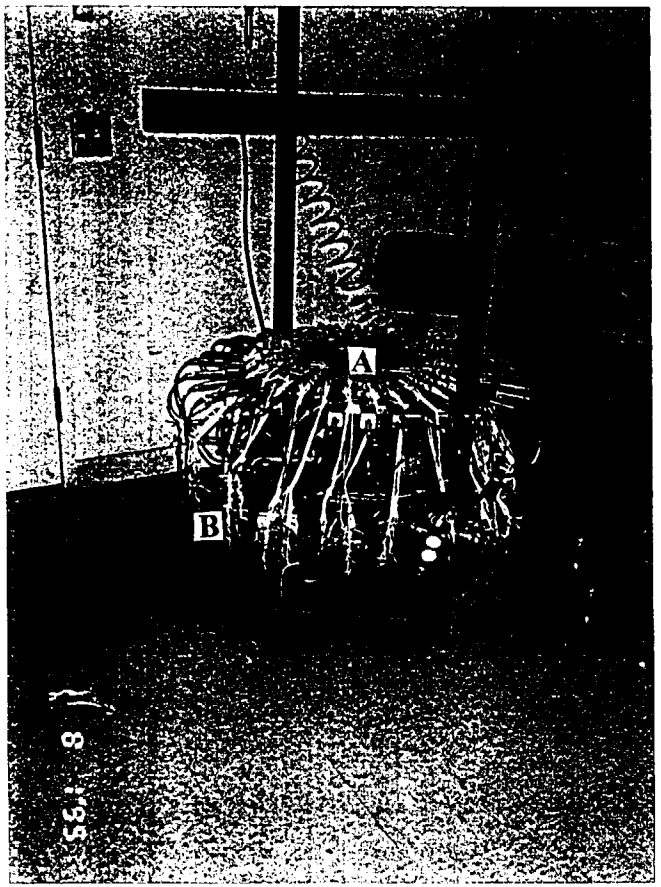

Figure 2.1 - Carrier being setup.

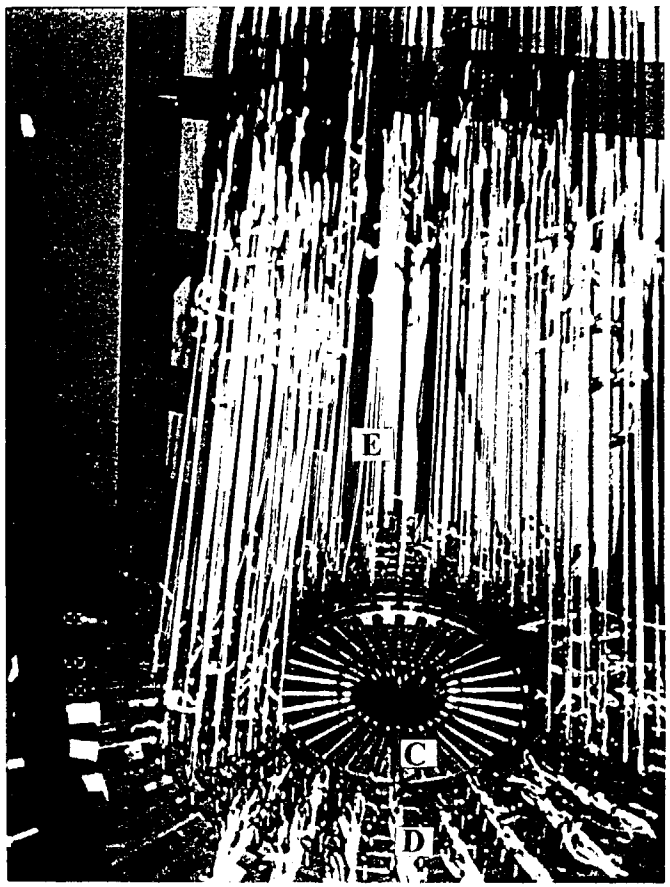

Figure 2.2 - Carrier being setup.

A - Carrier base
B - Green yarns tied to white elastic bands
C - Pneumatic carrier actuators
D - Unused carriers
E - Carriers tied to elastic bands, yarns, and fiber tows

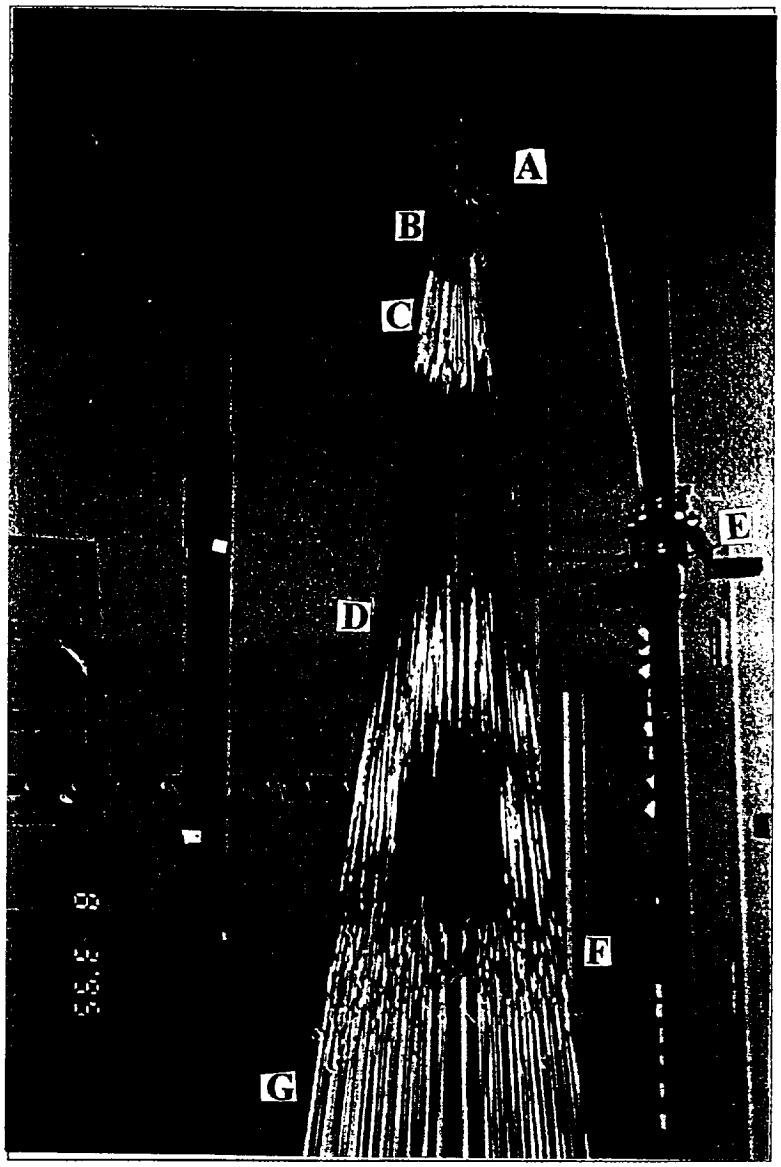

A - Two pulley system
B - Tow holder
C - Yarns taped to fiber tows
D - Fiber tows
E - Tensioning winch
F - Yarns taped to fiber tows and tied to elastic bands
G - Elastic bands

Figure 2.3 - Braiding Nomenclature. Picture taken at North Carolina State University.

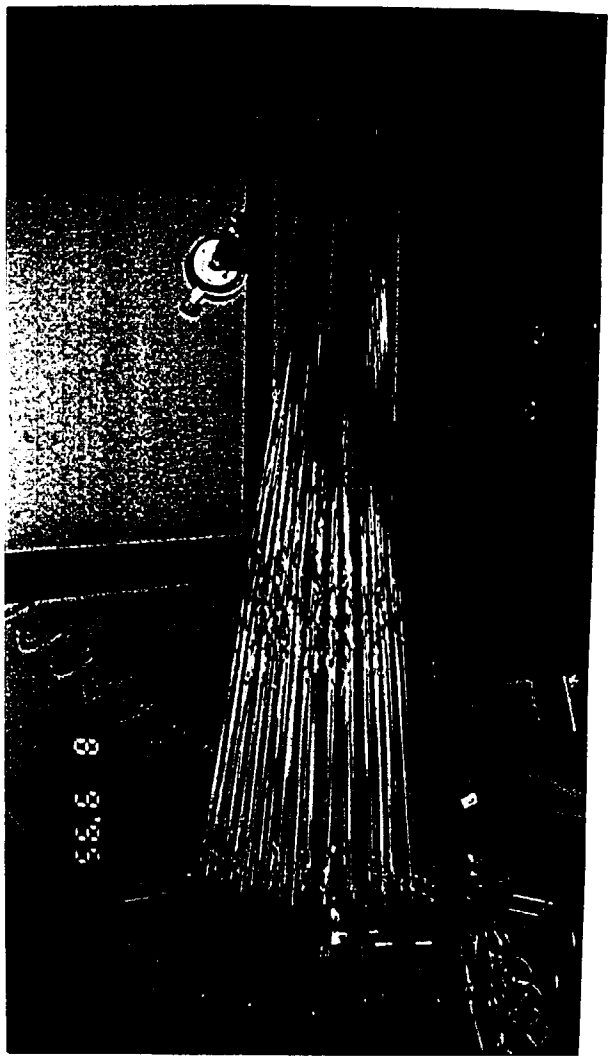

Figure 2.4 - Carrier partially setup

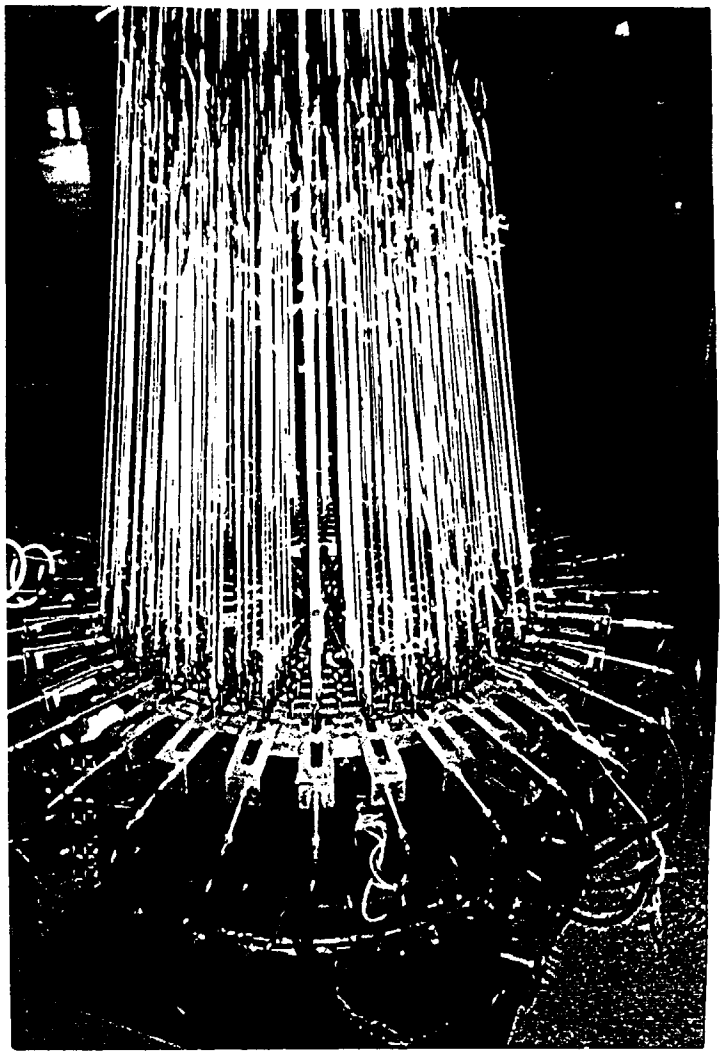

Figure 2.5- Finished carrier setup.

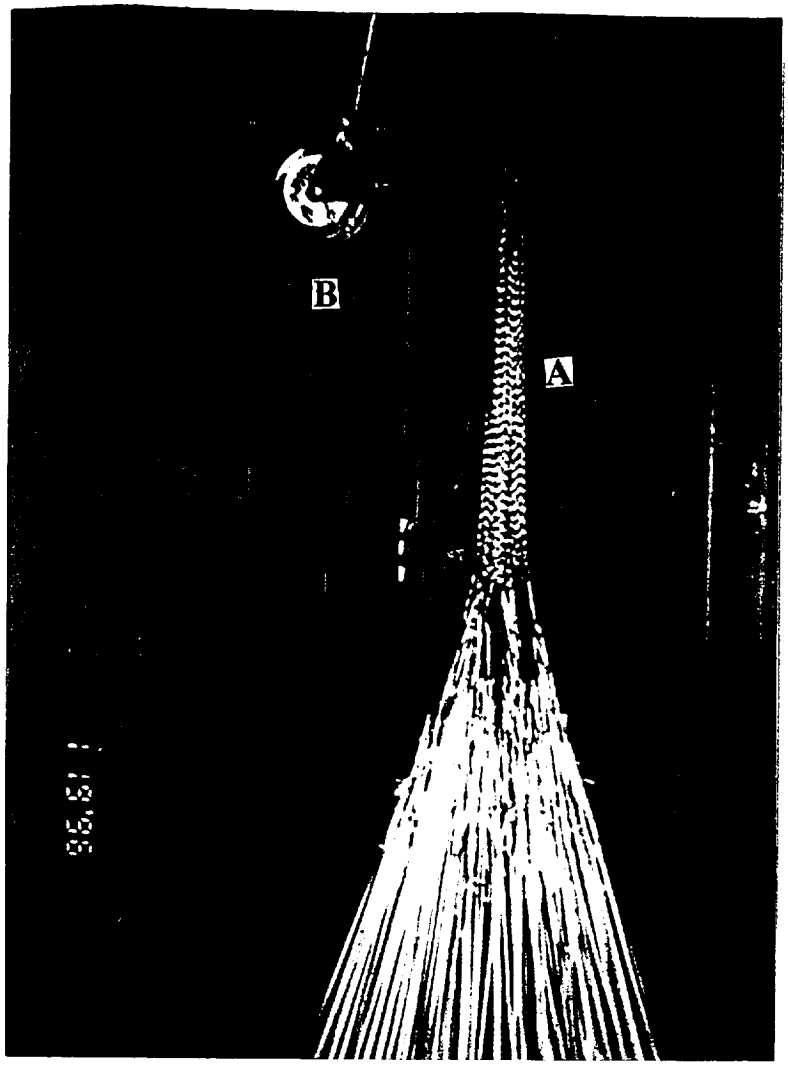

A - Finished 3-D braided 4 step finned tube preform

B - Tensioning winch

Figure 2.6 - Finished 3-D braided P100 HTS preform. Picture taken at North Carolina State University.

Table 2.1. Summary of attempted fiber materials and configurations.

Fiber Type	Tensile Strength	Elastic Modulus	Thermal Conductivity	Braidability
AS4	0.5 Msi	35 Msi	5.3 Btu/Hr ft F°	good
HMU	0.4	55	5.1	fair
P100	0.33	110	300	not braidable
P100 HTS	0.59	105	225	poor
K-1100 X	0.43	145	>1000	not braidable

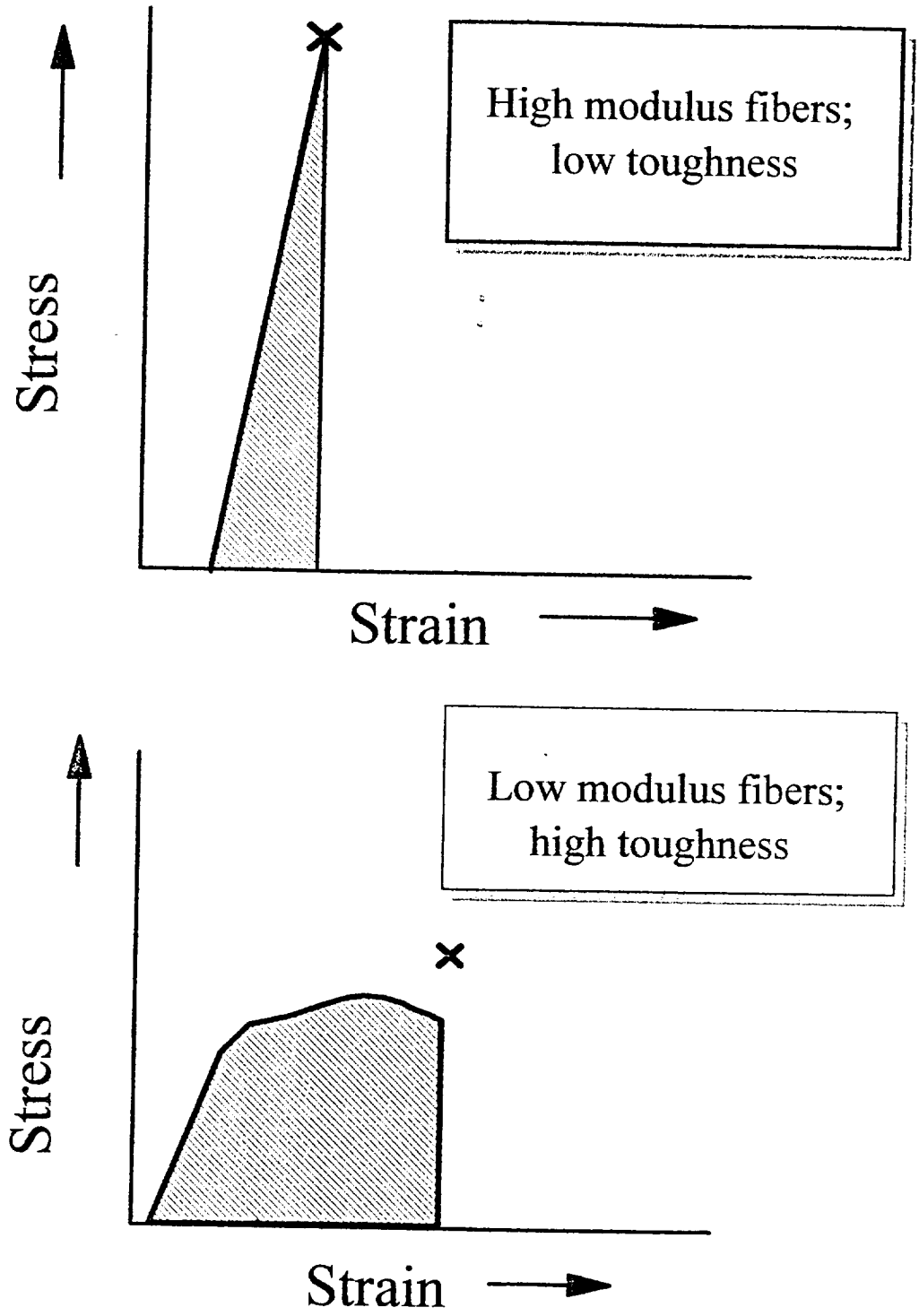

Figure 2.7 - High modulus vs. low modulus fibers. Toughness is given as area under the curve or the amount of energy absorbed before failure point **x.**

before failure or the area under the curve. Therefore, a high modulus, very stiff, material will have a very low toughness and fiber breakage can be expected to occur. Where as, a low modulus, ductile material, will absorb a greater amount of energy and fiber breakage is not as prevalent. The relationship between the stiffness to the toughness is summarized in figure 2.8a. In this figure, it is seen that as the toughness increases the stiffness decreases and vice versa. In order to braid a material, the ends of the tows have to be connected to the components of the braiding machine. These tows are tied to elastic stings by using knots. This itself is a severe process for the high modulus material and it causes an extreme increase in fiber breakage. Figures 2.9 -2.10 depict fiber breakage in the manual braiding process. Using the trends of the stiffness versus toughness given in figure 2.8a, the difficulty of braiding the desired material can be forecast.

Inter-tow friction reduces the braidability of a material by lowering toughness at the points of frictional contact in the fibers. When a preform is being fabricated, the tows rub against each other causing the fibers to fray or shed. Once fraying occurs, there are fewer fibers to absorb the energy due to handling and bending of the fibers. This causes a decrease in the overall toughness of the fibers and stress concentrations at the frayed points. These stress concentrations and frictional contact points can cause fiber breakage during the beating up process because the fibers can not absorb the energy created by friction and high stress concentrations between the fiber surfaces.

In order to obtain the desired braid angle in a perform, the preform has to be beaten up.

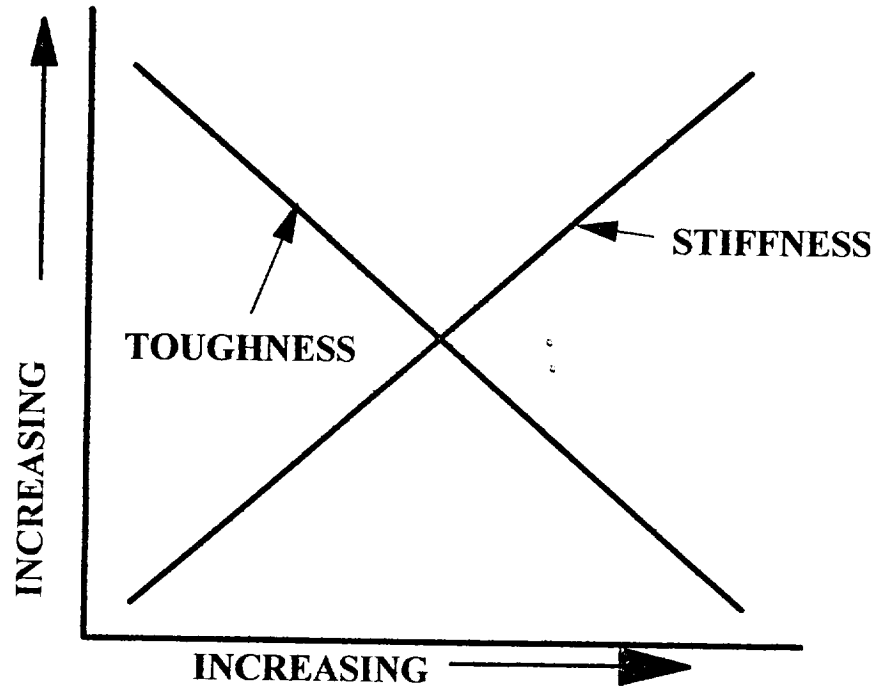

Figure 2.8 a - Trends of graphite fibers

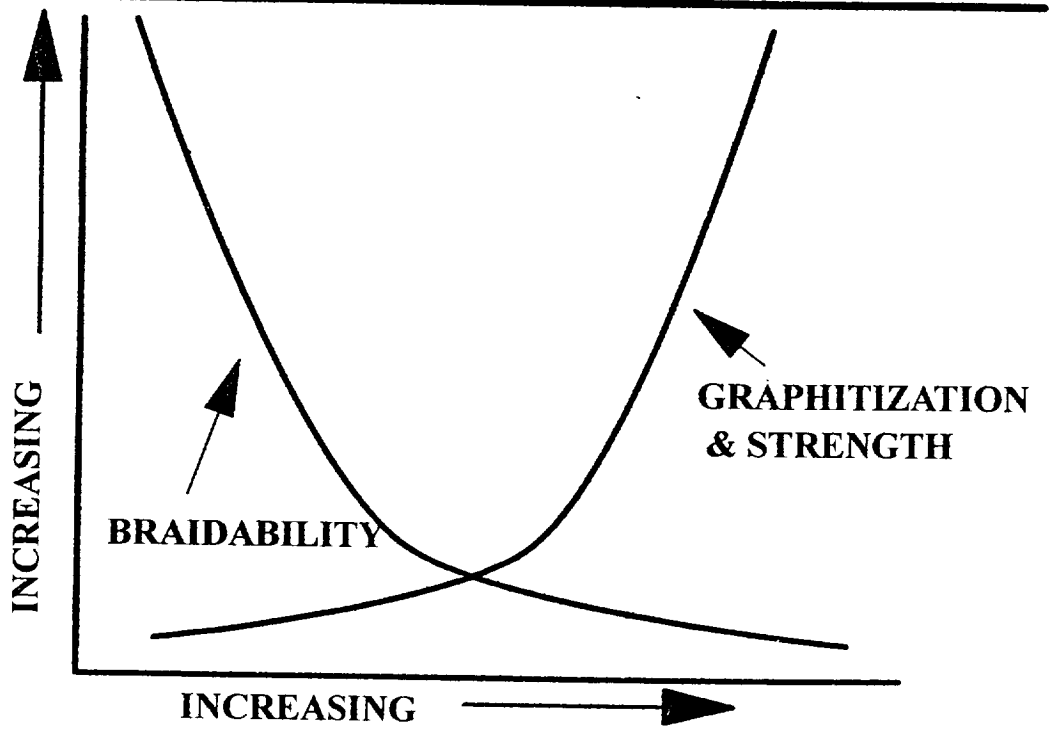

Figure 2.8 b - Braidability vs. Graphitization

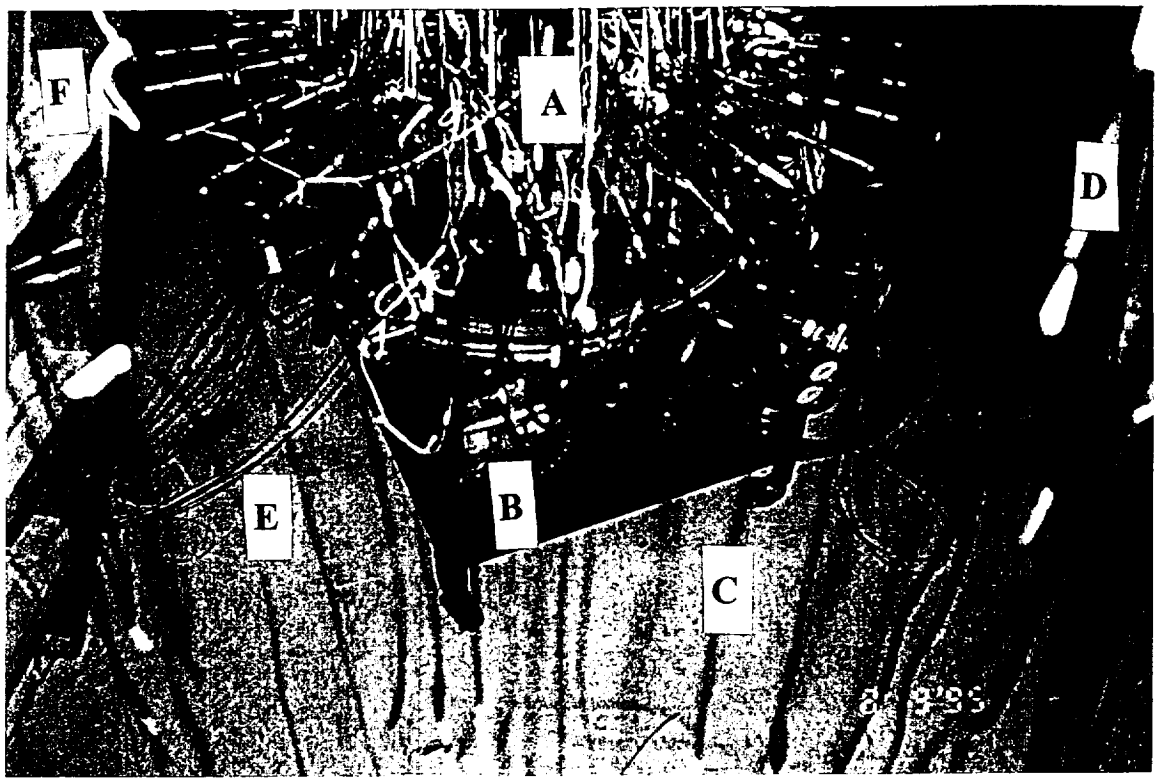

A - Carrier holders with white elastic bands

B - Switches for pneumatic actuators

C - Broken tows on ladder

D - Yarn taped to broken tows

E - Broken tow on floor

F - Ladder

Figure 2.9 - Shows fiber breakage.

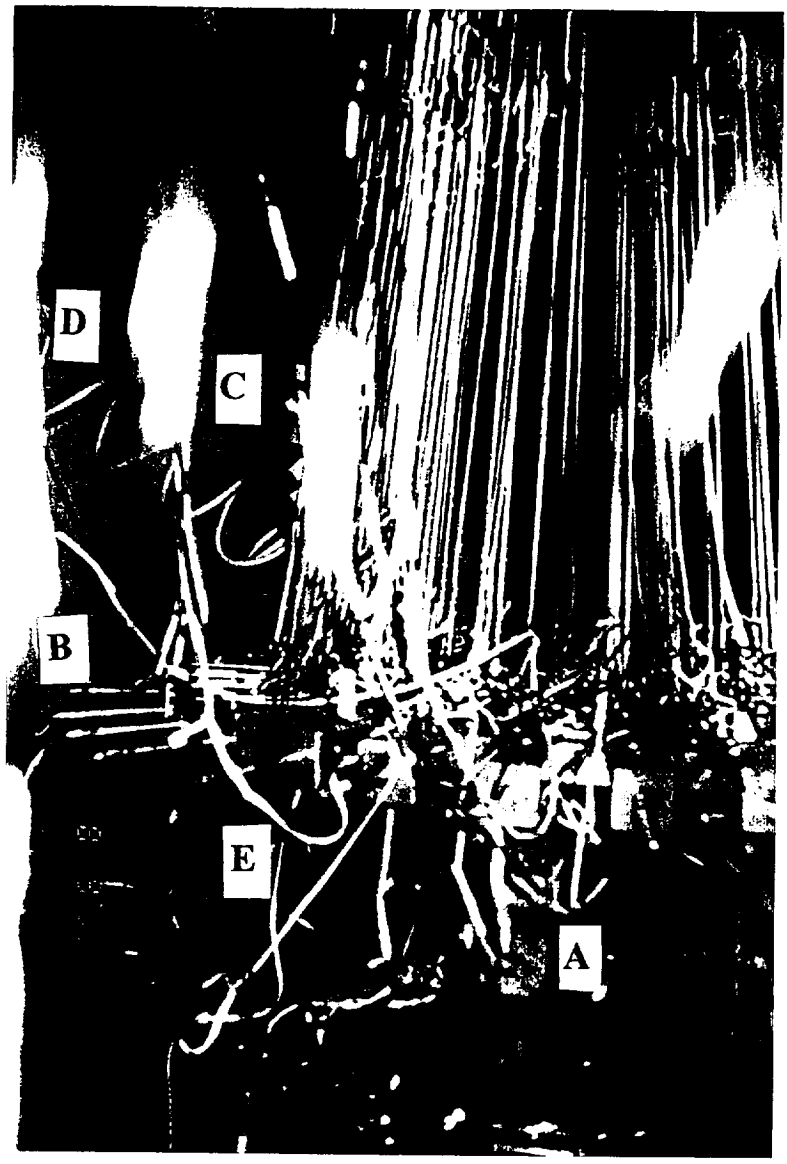

A - Broken fiber yarn taped to elastic strips
B - Pneumatic actuators
C - Broken fibers hanging from tow holder
D - Air tube
E - Elastic bands tied to broken fiber tows

Figure 2.10- Shows fiber breakage. Notice the tows on the floor.

During this process, the tows are pushed outward and the beating stick is used to compact the tows at the vertex of tow angles. This is repeated until the angle measurer reads the desired braid angle. The beating up process is shown in Figure 2.11. Notice that tows are subjected to bending during this process. The amount that a tows is required to bend is determined by the braid angle. Figure 2.12 compares the low and high braid angles relative to the beating up process. If a high braid angle is desired, the tows have to be pushed outward and compacted. Where as, to obtain a low braid angle the beating up process is not as severe. For this reason, braiding high modulus materials is difficult and fiber breakage often occurs . The beating up process has to be repeated after each braiding cycle. Since a manual braiding machine was used in this research, variability occurs in the braid angles from cycle to cycle. As the skill of the braider increases, the preforms become more uniform.

The braidability of a material is contingent upon its mechanical properties and the phenomena of fiber breakage, inter-tow friction, and the beating up process. Hence, the only way to increase the braidability of a material is to alter braiding parameters since the mechanical properties can not be altered. In order to braid high modulus materials, the end of the tows were taped to yarns which were tied to the elastic strips on the carrier and tow holder, thus decreasing the forces due to bending produced from tying knots in fibers. Figures 2.1- 2.6 show the fibers tows taped to yarns. It is important to notice that even though taping the fibers to yarns does increase the braidability, there was still some fiber breakage as shown in figures 2.9 and 2.10. The braidability can also be increased by

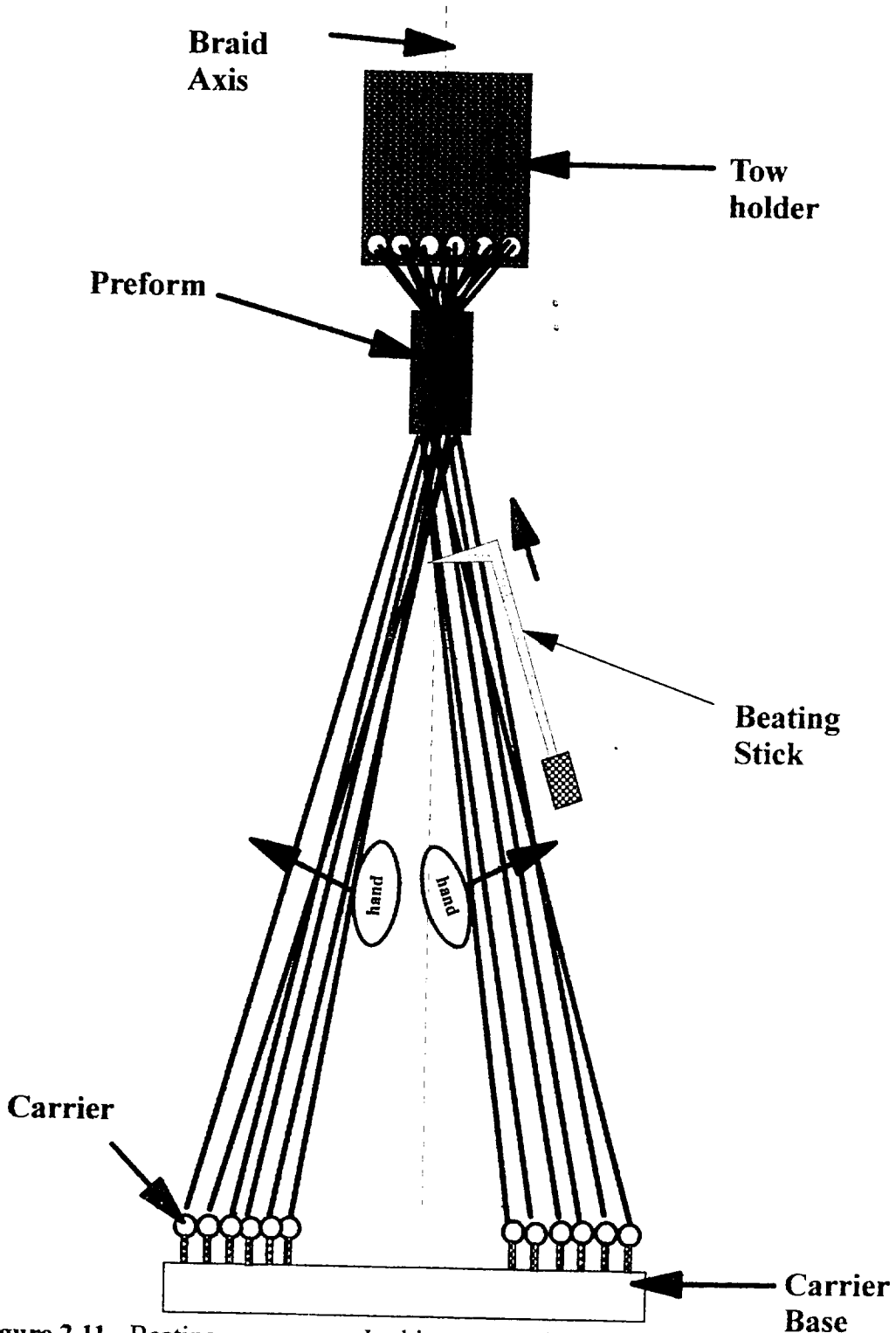

Figure 2.11 - Beating up process. In this process, the hands push the tows outward and the beating stick is used to compact the vertex of the desired braid angle.

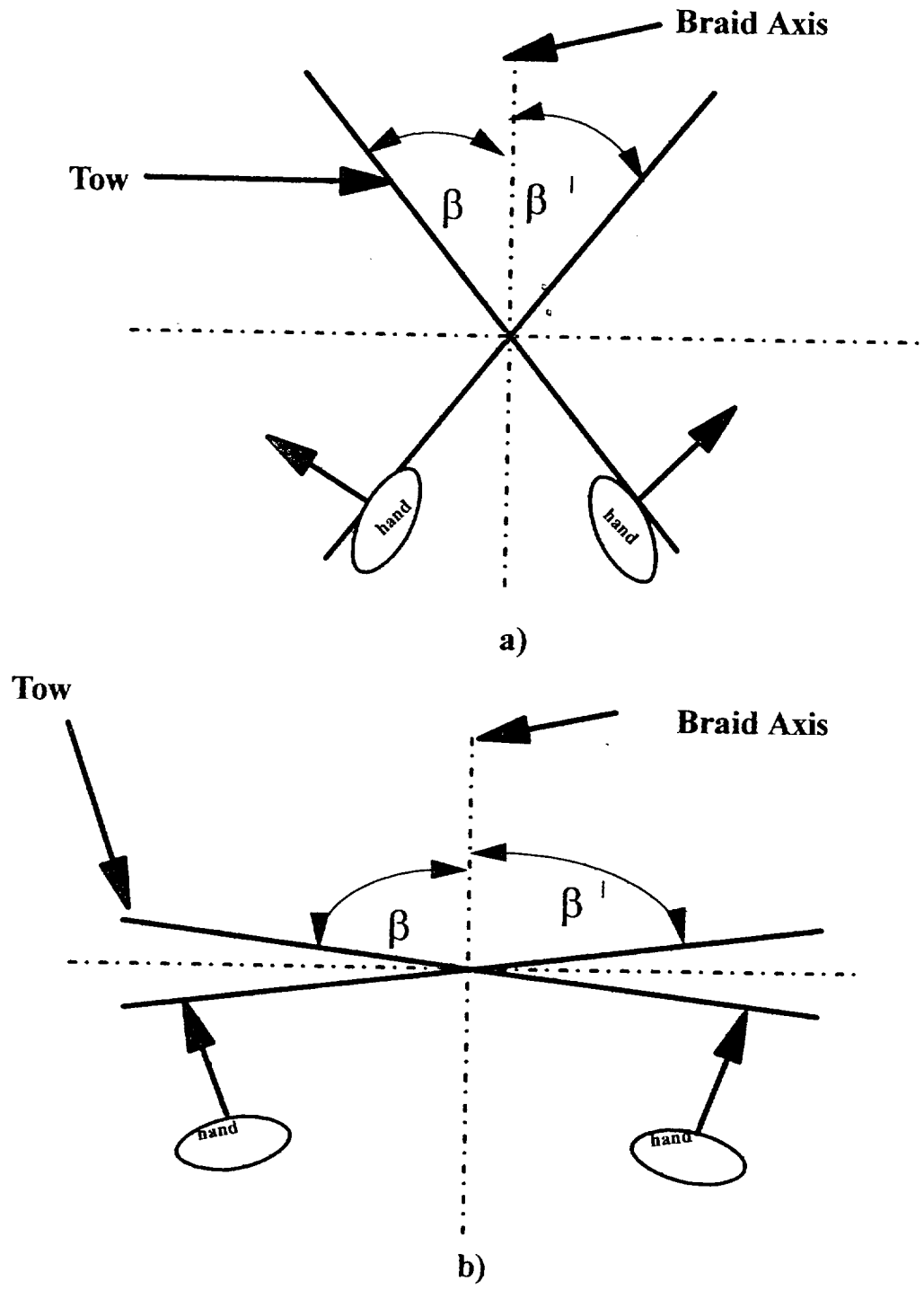

Figure 2.12 - Shows the comparison of a large braid angle in b to a small braid angle in a. Notice that the larger braid angle requires more bending of the fibers as described in figure 2.5.

using lubricants such as water to lower the inter-tow friction. The lubricant is applied just before the beating up process is started after each cycle (1cycle = four steps). The braidability also increases when a lower braid angle is used during the beating up process so that excess bending of the fiber does not occur. The final way to increase the braidability of a material is if the material could be graphitized after the braiding process is finished. This is a very expensive but extremely effective process. If this process is used, the P100 HTS fibers that were used in the research could be graphitized to the K1100-X fibers increasing the conductivity. The details of this process are not available, but the implications of this process are considerable.

Figure 2.8b shows the braidability trend. This figure shows that as the graphitization and strength increases, the braidability decreases. These relationships indicated that the material that was originally considered, K-1100 X, can not be braided even with the above modifications. In order to get the best possible material, P100 HTS was used instead of the K-1100 X fibers. Although the P100 HTS has a similar thermal conductivity to copper, it still offers large advantages of strength to weight ratio, more rigidity, and a higher operating temperature than pure OFHC copper. Unlike the more thermally conductive P100 fibers which are extremely brittle and not braidable because fiber breakage can not be controlled, the P100 HTS fibers have been treated with a special toughening process that enables braiding. Analysis of table 2.1 shows that the tensile strength of P100 HTS fibers are higher than that of P100 fibers and they still offer more ductility than P100 fibers. Therefore, the P100 HTS fibers were found to be

a suitable replacement for the K-1100 X fibers.

2.2 Carrier Motions of Braiding Machine

In figures 2.1- 2.6 the braiding machine can be seen with elastic bands tied to yarns that were tied to the carrier. These carriers are responsible for the braiding process. The carriers braid the preform by moving radially along columns and circumferential along the rings and/or rows on the base. Pneumatic cylinders cause the carriers to move one carrier radially or rotate one carrier over. In order to specify how many rotating rings or transversely moving rows and columns in a braiding structure, the term **mxn** braiding pattern is used (Hammad). In tubular braiding, the number of rotating rings is specified as **m,** and the number of columns is specified as **n**. In transverse braiding of the fins, the number of moving rows is specified as **m**, and the number of full columns is specified as **n**. In this research, the fins were 2 x 14, two transversely moving rows by 14 columns, and the tube was 2 x 30, two circumferential rotating rings by 30 radially moving columns. The carrier motions to braid the fins can be seen in figure 2.13 and the tube carrier motions can be seen in figure 2.14.

As the carriers create the preform, an interesting sequence is noticed. Some of the carriers move in the same braiding patterns. The name given to carriers that move along the same braiding patterns is braider groups. Understanding the braider groups allows the braider to setup the carrier to produce different configurations. Figure 2.15 shows the braider groups of the fins and tube. Notice if the numeric or alphabetical order is

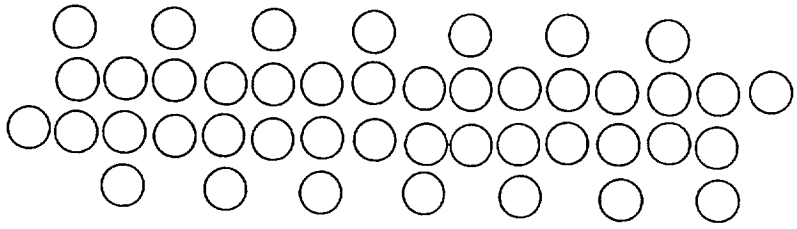

Original Position

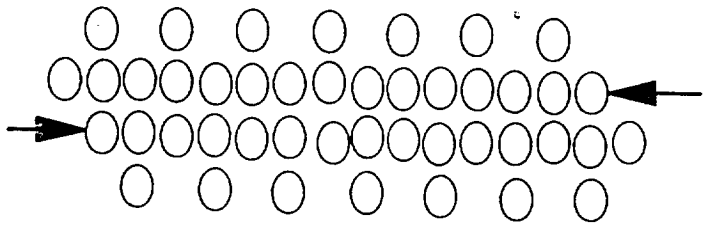

After step 1

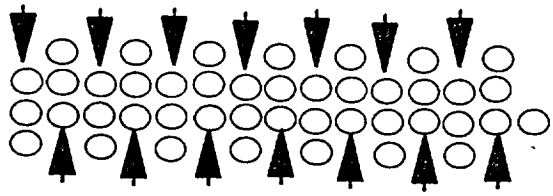

After step 2

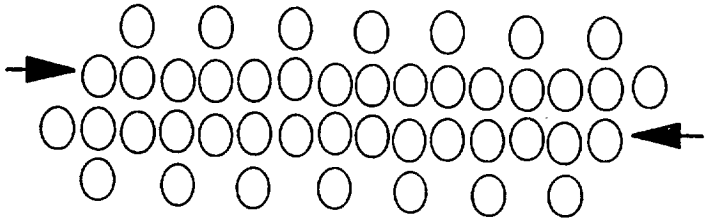

After step 3

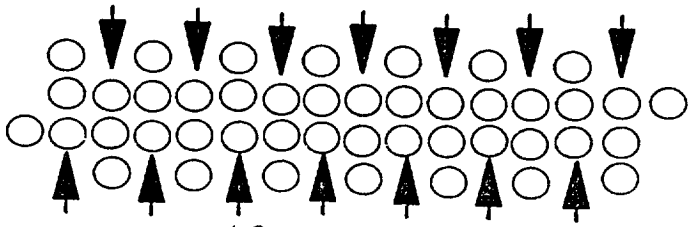

After step 4

Figure 2.13- Carrier motions for four step 2 x 14 fins.

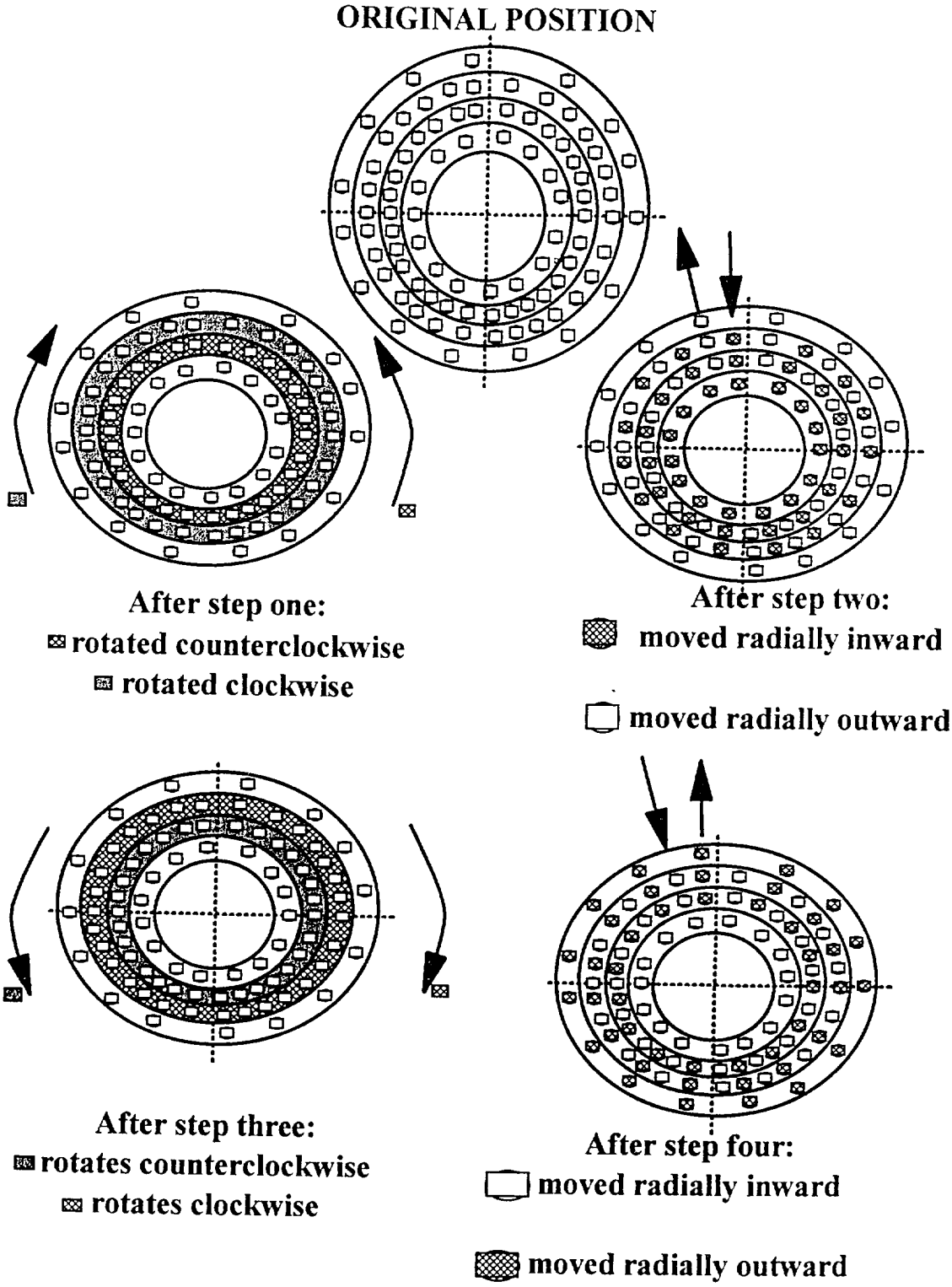

Figure 2.14 - Carrier motions for 2 X 30 four step tube

followed the braiding pattern can be established. In the case of the tube, notice that one braider group braids clockwise and the other counterclockwise. The important fact is that all the braiders groups are moving simultaneously. In addition, it takes four steps for a carrier to move from one position to the next. For this reason, the braided preform has a four step braiding pattern. In order to find out how many steps it will take to move through the fin or the tube, the number of total positions plus one must be multiplied by four since there are four steps to each position. Thus, a carrier must go through 22 braider group positions for each braider group with a total of 184 steps per fin, and 45 braider group positions for each braider group with a total of 368 steps for the tube. Once the carriers have completed these braider group positions and steps they are back in their original position and one structural repeat is formed. The total motions for the fin and tube can be seen in table 2.2.

In order to braid a finned tube, a relationship of the fins to the tube must be established. By transforming the transverse motions of the fins onto a circular carrier a finned tube was braided. Original carrier motions are shown in figure 2.16. The first three rings of the carriers braid the tube, while the last three braid the fins. Ring four is shared between the fins and the tube. The carrier motions for the finned tube are shown in figures 2.17 - 2.20.

Analysis of these figures reveal that the carrier motions for steps one through four are exactly the same as the individual carrier motions for the fin and tube. However, steps five through eight are simply to connect the fin to the tube. This allows the fin tube to be

Table 2.2 Summary of m x n braiding structure

COMPONENT	Moving Rows or Rings (m)	Moving Columns (n)	Braiding Structure (mxn)	**Total Moves Required for Structural Repeat
Fin	2	14	2 x 14	184
Tube	2	30	2 x 30	368
Finned Tube	5	30	**Combined** 2 x 14 & 2 x 30	552

Total # of moves for structural repeat =

(Total # braiders in braider group)* # Steps in the process

a) Left fin

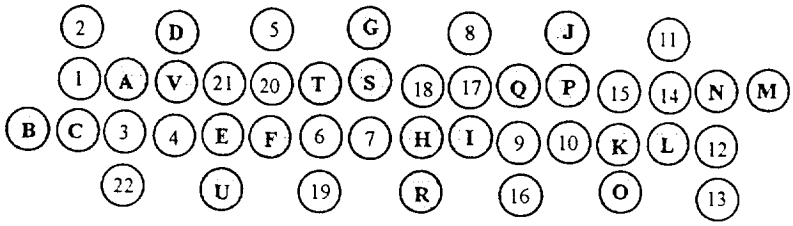

Braider Group 1 Braider Group 2

b) Right fin

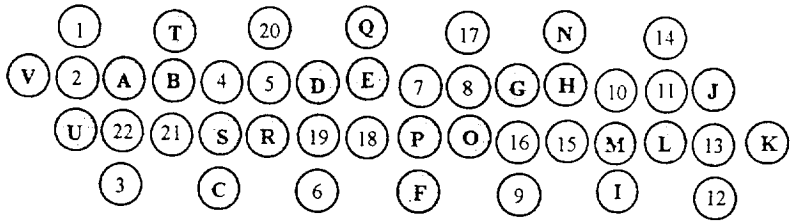

Braider Group 1 Braider Group 2

c) Tube

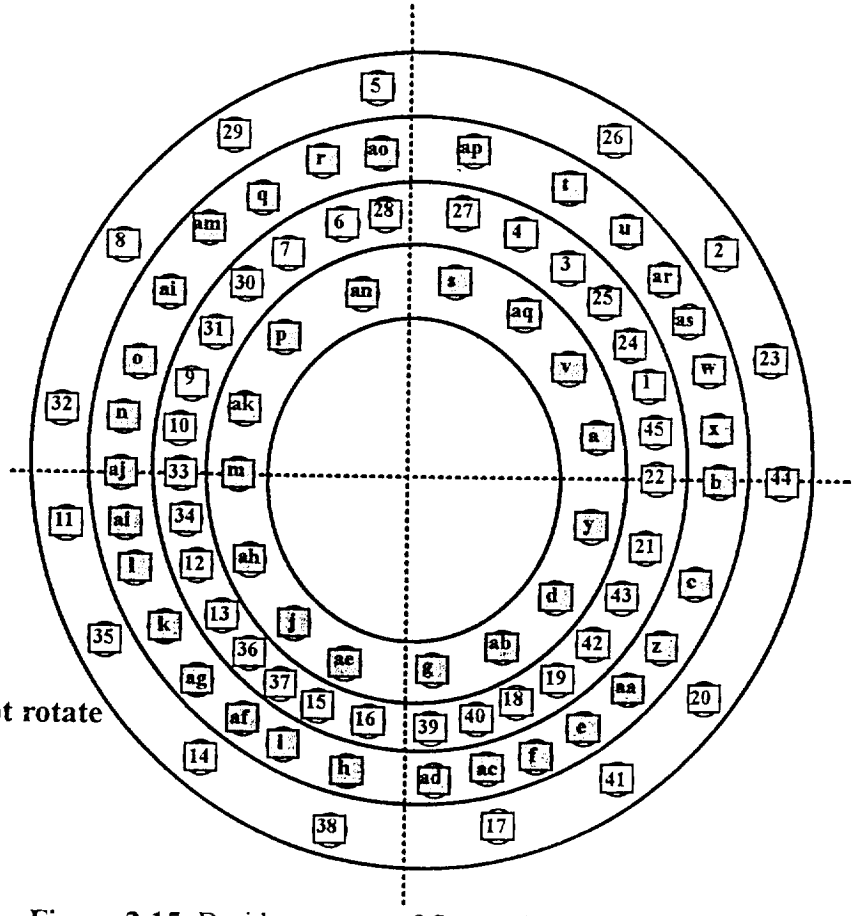

Braider Group 1

Braider Group 2

* Rings 1 and 4 do not rotate

Figure 2.15 Braider groups of fins and tube

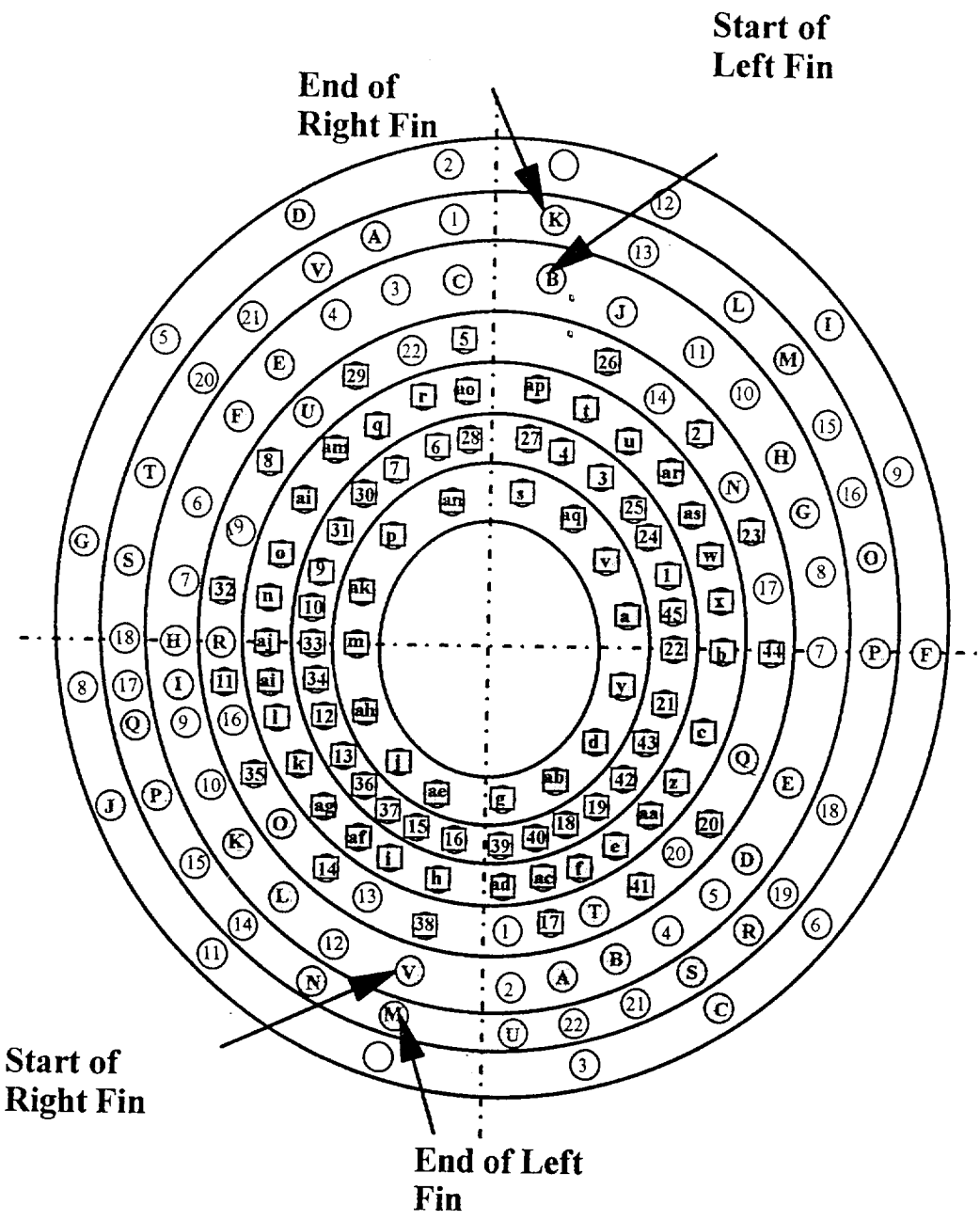

Figure 2.16- Original position of carrier motion setup for finned tube. Braider groups are the same as in previous figures depicting fin and tube carrier motions and are not drawn to scale. The first three rings are setup to braid the tube and the last three rings are setup to braid the fin. Ring four is shared between the fin and tube.

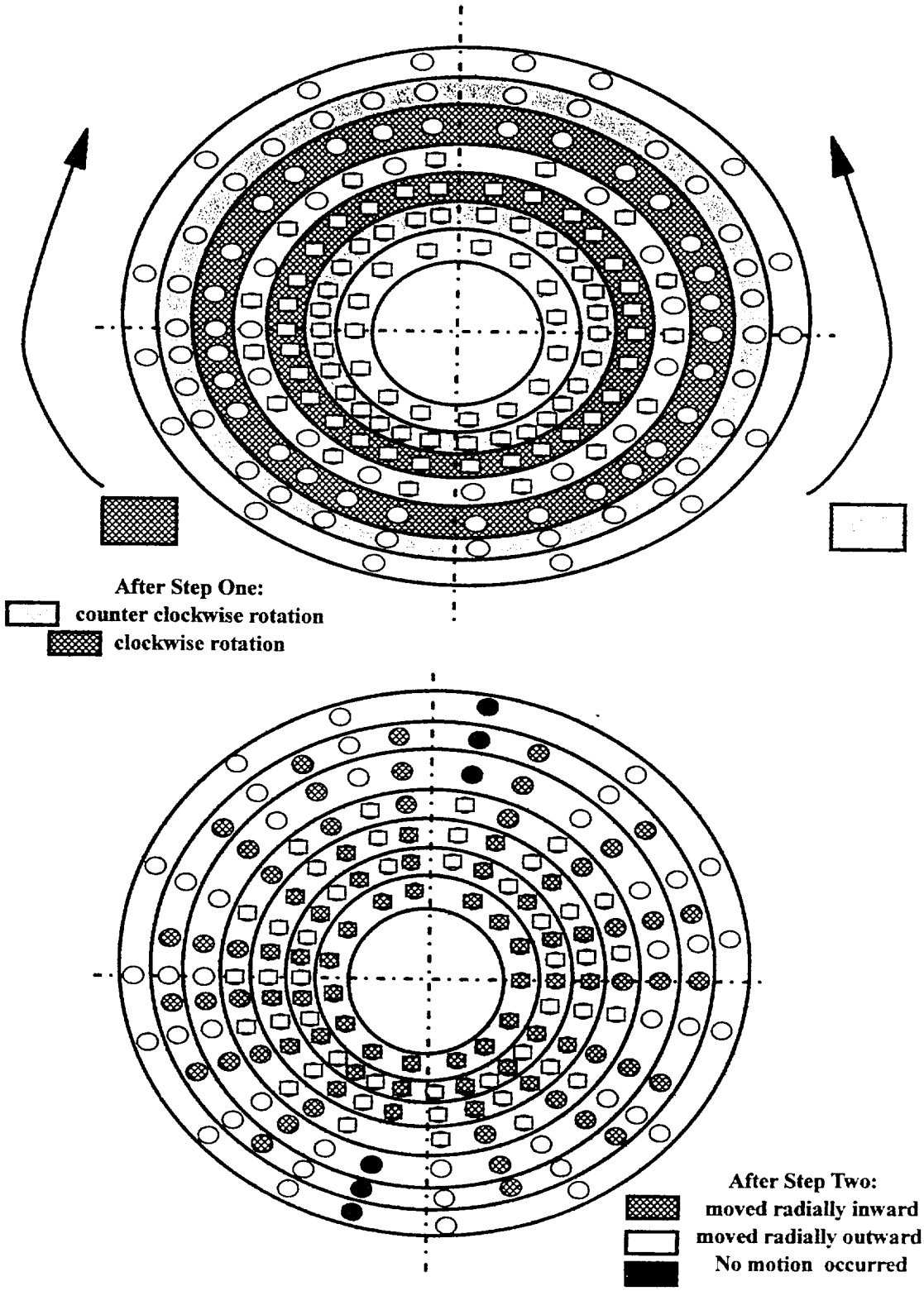

Figure 2.17 - Carrier motions 1- 2 for finned tube

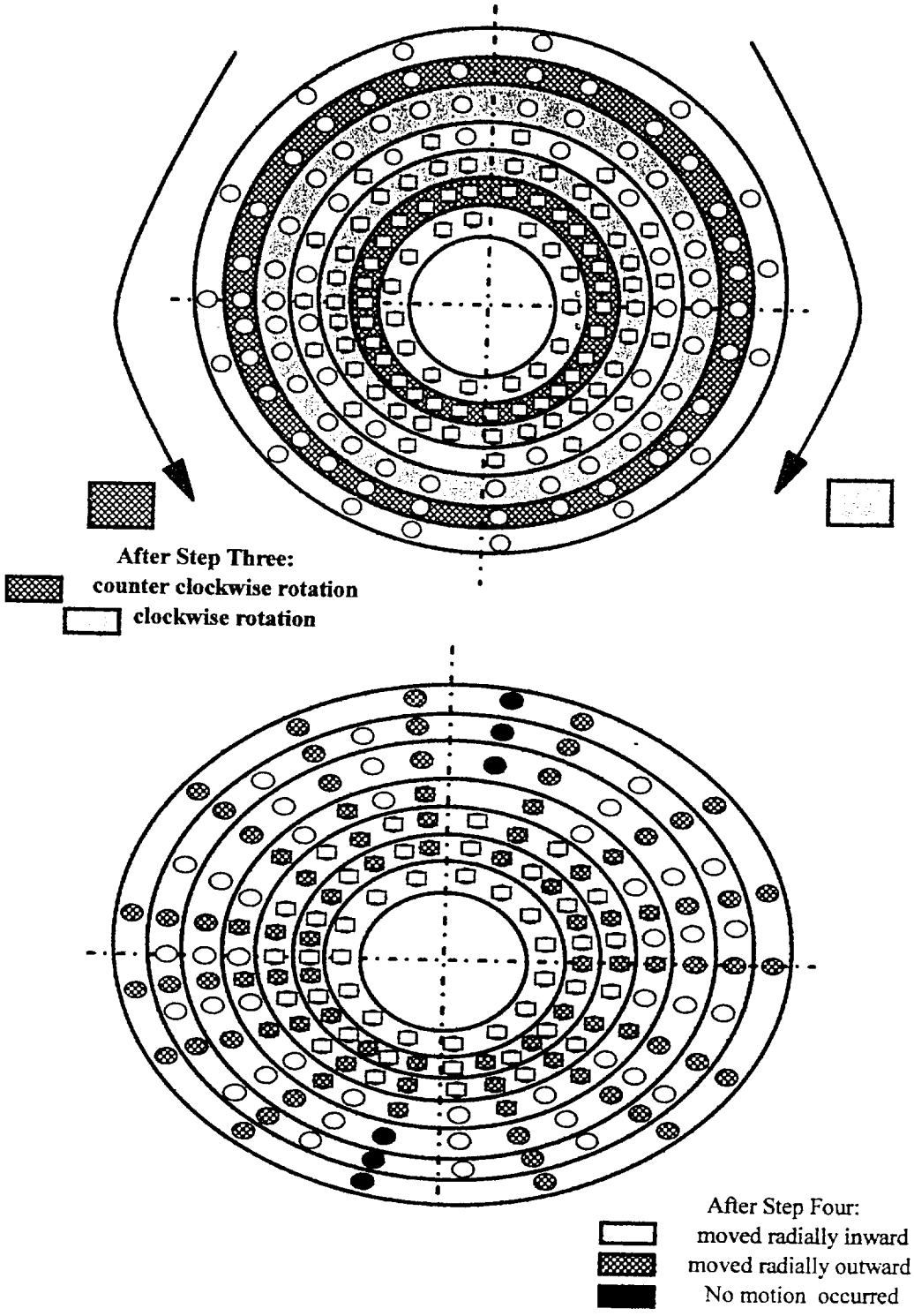

Figure 2.18 - Carrier motions 3-4 for finned tube

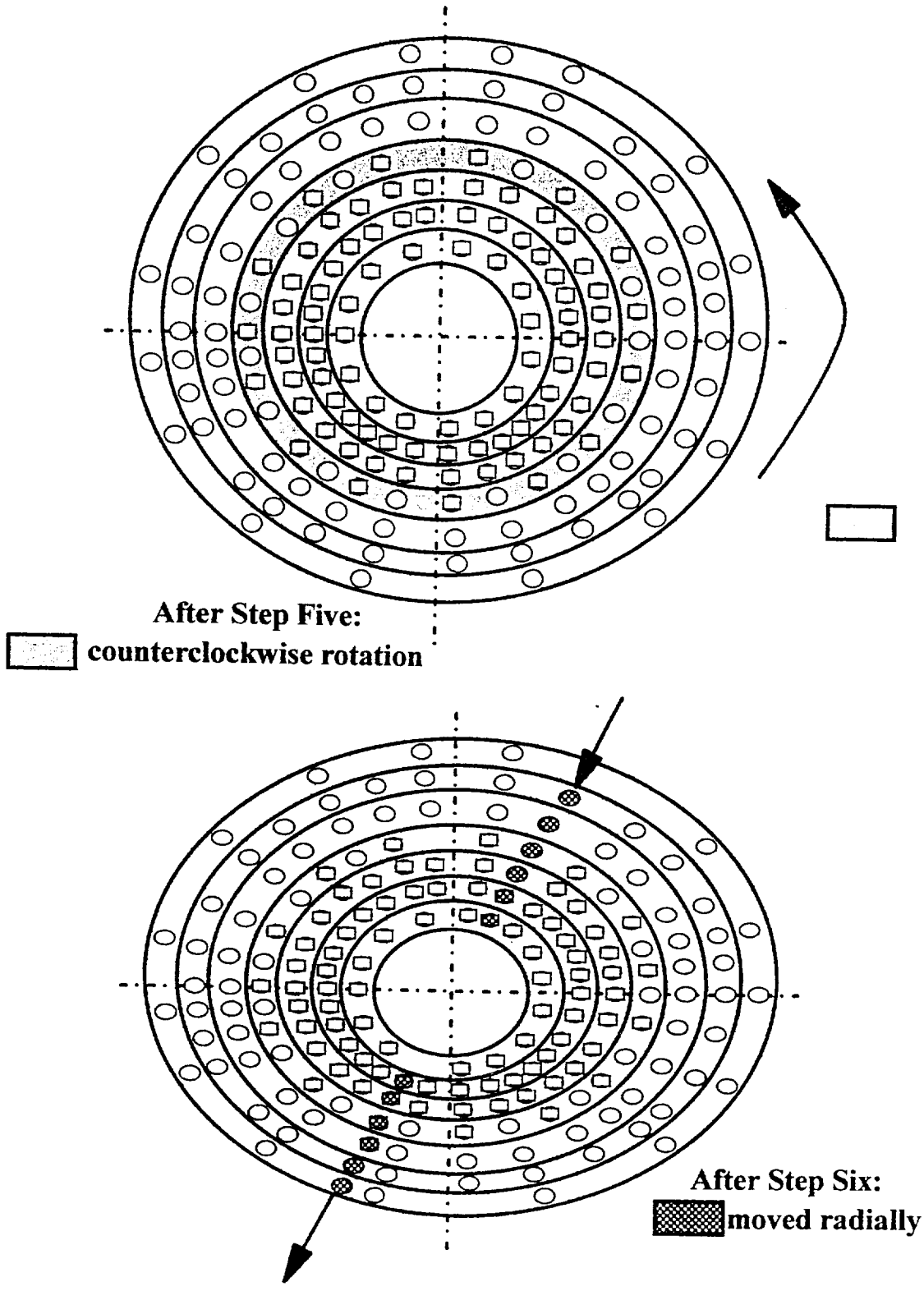

Figure 2.19- Carrier motions 5-6 for finned tube

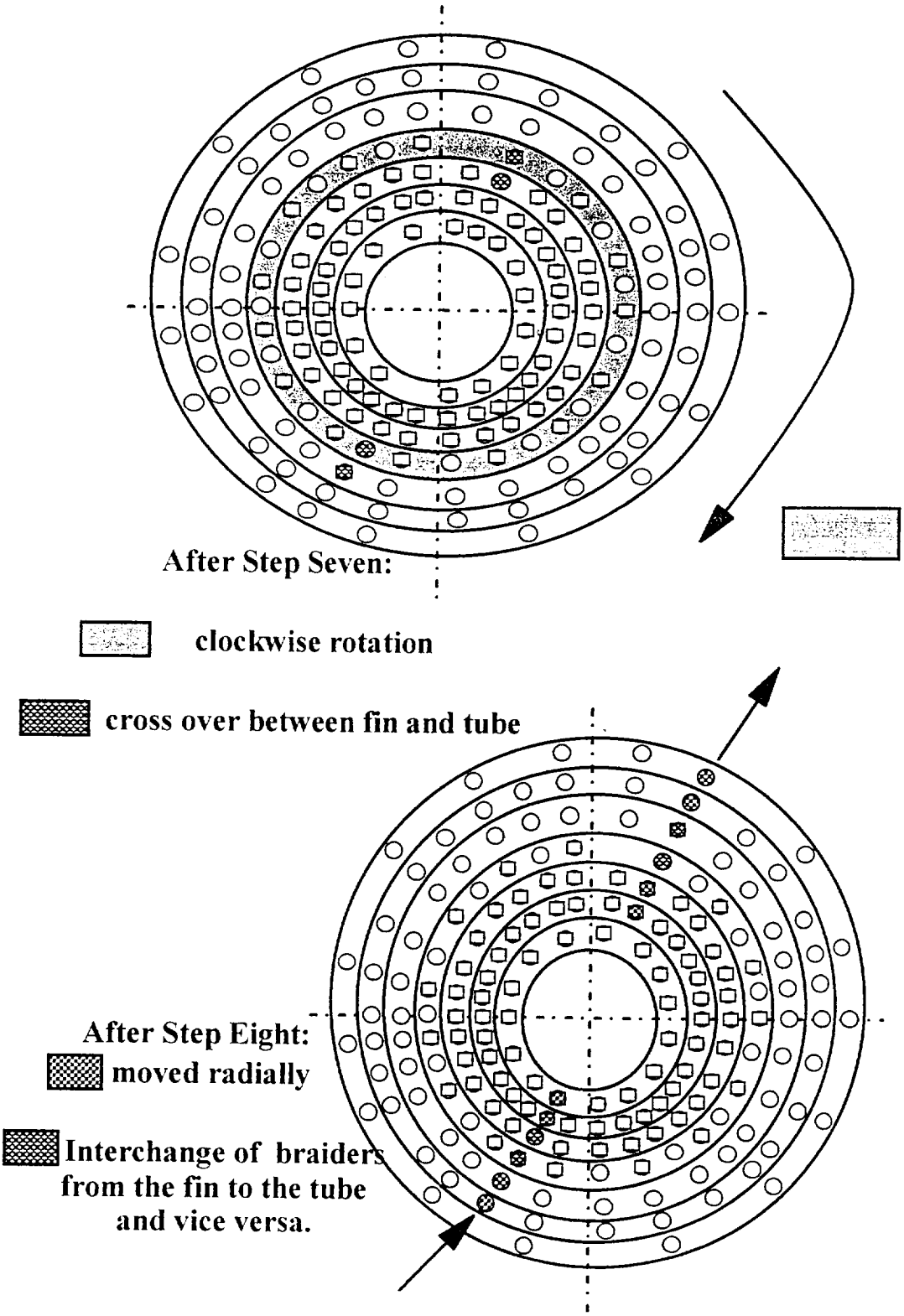

Figure 2.20 - Carrier motions 7-8 for finned tube

an integral part. Notice at step seven the fin and the tube exchange carriers. This now means that the tube carrier will go through all 44 (moving through both braider groups with 22 in each braider group) braider group positions of the fin before it returns to the tube, and the fin carrier will braid over until it reaches the other fin. Upon reaching the other fin, the fin carrier will then go through the 44 braider group positions of the other fin then it will exchange with the tube carrier again and braid through the preform until it exchanges to its original position. At this point, a structural repeat is formed. These motions are shown in the structural map of the braided finned tube preform in figure 2.21. This figure shows the braid angles α, β, δ. These braid angles are shown as braiding planes, planes at which the tow travels throughout the preform. Ideally these three angles should be equal, but due to variability in the braiding process and the skill of the braider these angles vary. The angle at which the tows travel through the preform on the braiding planes, α,β,δ, is γ. γ also varies because as the braiding angles change, so does γ. Ideally there should be four values for γ which come from each of the changes in the tow planes. Conversely, for the braider groups of the tube that are braiding clockwise, the structural map would spiral down in the opposite direction.

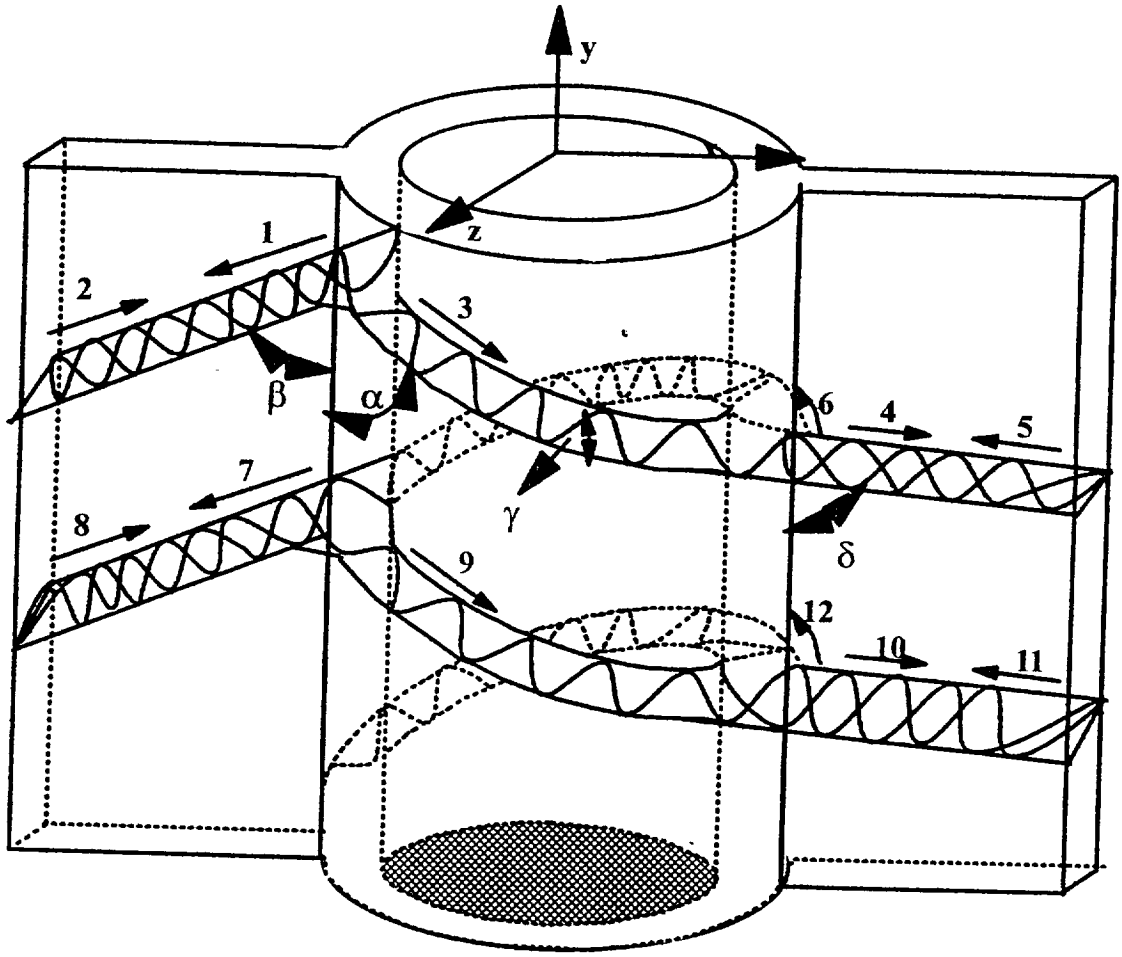

α, β, δ - are the braid angles. Ideally, these angles are equal.

γ - is the angle that tows travel throughout the preform. There are 4 ideal values for γ . γ varies because of the variability in the braiding process. The numbers and arrows represent the braiding directions. See Table 2.3 for further explanation.

Figure 2.21 - Structural map of braided finned tube preform

Table 2.3 Summary of braiding pattern directions

Position Number	Explanation
1	Braiding from outer diameter of tube to outer edge of left fin
2	Braiding from outer edge of left fin to outer diameter of tube
3	Braiding circumferentially around the front of the tube
4	Braiding from outer diameter of tube to outer edge of right fin
5	Braiding from outer edge of right fin to outer diameter of tube
6	Braiding circumferentially around the back of the tube
7	Braiding from outer diameter of tube to outer edge of left fin
8	Braiding from outer edge of left fin to outer diameter of tube
9	Braiding circumferentially around the front of the tube
10	Braiding from outer diameter of tube to outer edge of right fin
11	Braiding from outer edge of right fin to outer diameter of tube
12	Braiding circumferentially around the back of the tube

CHAPTER THREE

Treatment and Infiltration

3.1 Manipulation of the Preform

The nature of a 3-D braid is to stabilize itself by using interlocking tows. However, if the ends of preform are not held together the interlocks between the tows are destroyed and the preform unravels. For this reason, several methods were used to restrain the ends of the preform. Using a similar practice preform composed of HMU, the effects of handling the P100 HTS preform was simulated. The HMU fibers were chosen because they had a similar braidability to that of the P100 HTS fibers, and as shown in table 2.1 these fibers are the only suitable option from the materials chosen in the research. By practicing with the HMU fibers, the issues of material handling and preform final dimensions could be resolved.

Three approaches were taken in order to solve the problems of unraveling. The first of these approaches is sealing the preform with silicone rubber. This process worked and was used to restrain the HMU preform while it was being epoxy infiltrated. However, this process was not feasible for the infiltration of copper because when the proprietary plasma coating is applied to the fibers the silicon may form silicon carbides. The next process that was used was to melt candle wax on the preform ends. This process restrained the preform, but possible contamination of the plasma coating due to wax

removal heating would cause the fibers to wick throughout the preform. The final method involved sewing the preform with thin copper wire. The results of this process can be seen in figures 3.1 -3.3. This alternative would allow the copper wire to be coated with the plasma coating at 1000 °F and prevent the preform from unraveling.

3.2 Infiltration of HMU Preform

Infiltration of the HMU preform was performed to resolve issues relating to preform properties, volume fraction, and the prediction of the dimensions of the final copper infiltrated P100 HTS preform. Because the dimensions, braid angles, and volume fraction of the preform are interlinked, a change in one constitutes a change in the other. For this reason, trial and error had to be used in order to optimize the desired dimensions of the final component. The preforms fabricated from this procedure provided valid measurements for the final components overall thickness and inner and outer diameter.

Procedure for infiltrating HMU Preform with Epoxy

- ❑ Apply Mold release to the mold
- ❑ Prepare resin- Mixture Ratio:

$$\frac{\text{100 grams of Epon 828}}{\text{42 grams of Jeffamine T-403}}$$

- ❑ Degas the resin in vacuum chamber-to reduce voids
- ❑ Submerge preform on mandrel in degassed resin
- ❑ Place resin saturated preform in mold and seal with high temperature tape
- ❑ Cure preform in oven at 212 °F for 2 hours

Figure 3.4 shows the infiltration process for the HMU preform. The mold was

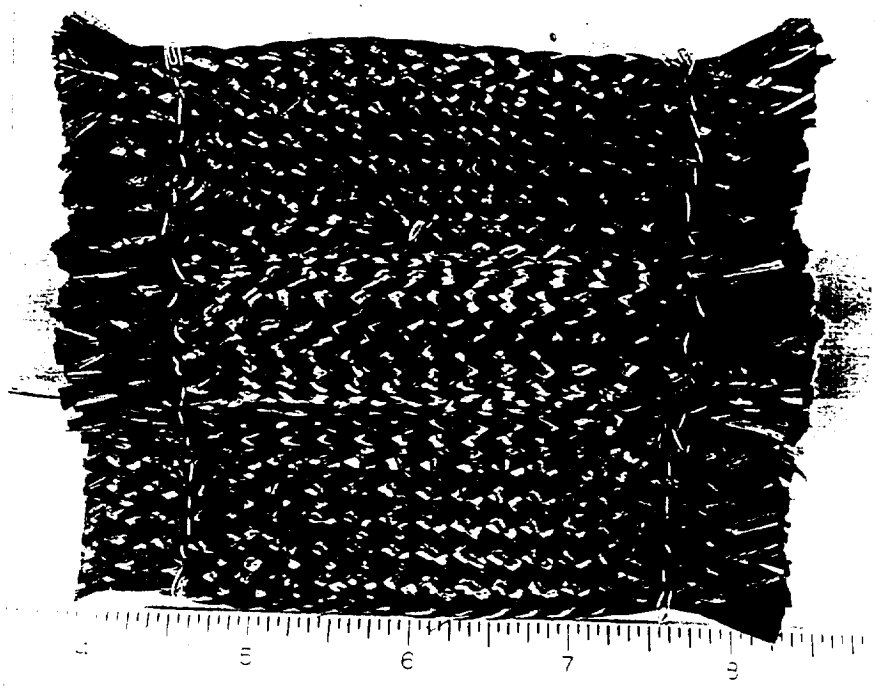

Figure 3.1 - Stabilization of preform

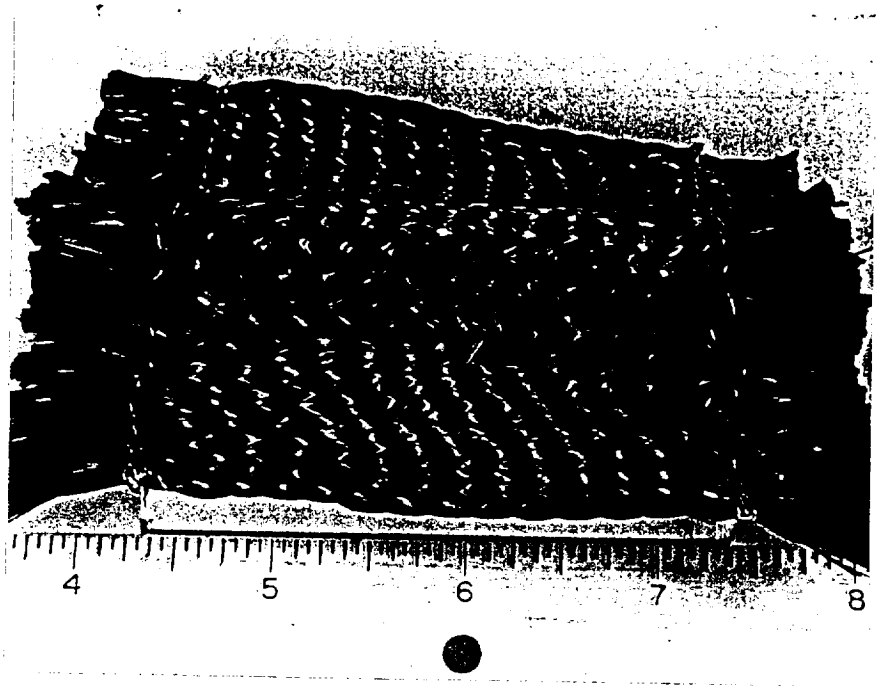

Figure 3.2 - Stabilization of preform

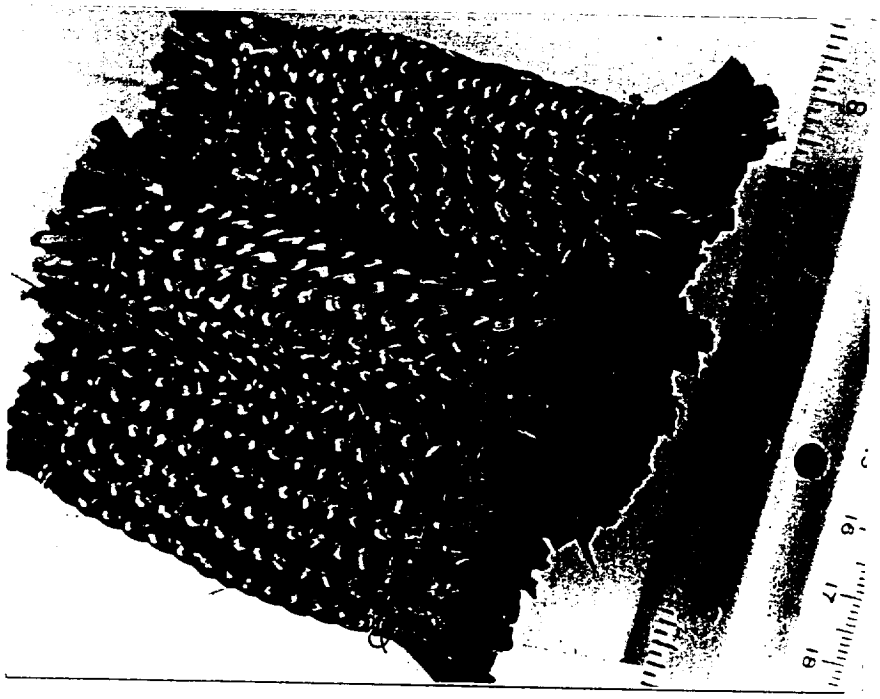

Figure 3.3 - Stabilization of preform

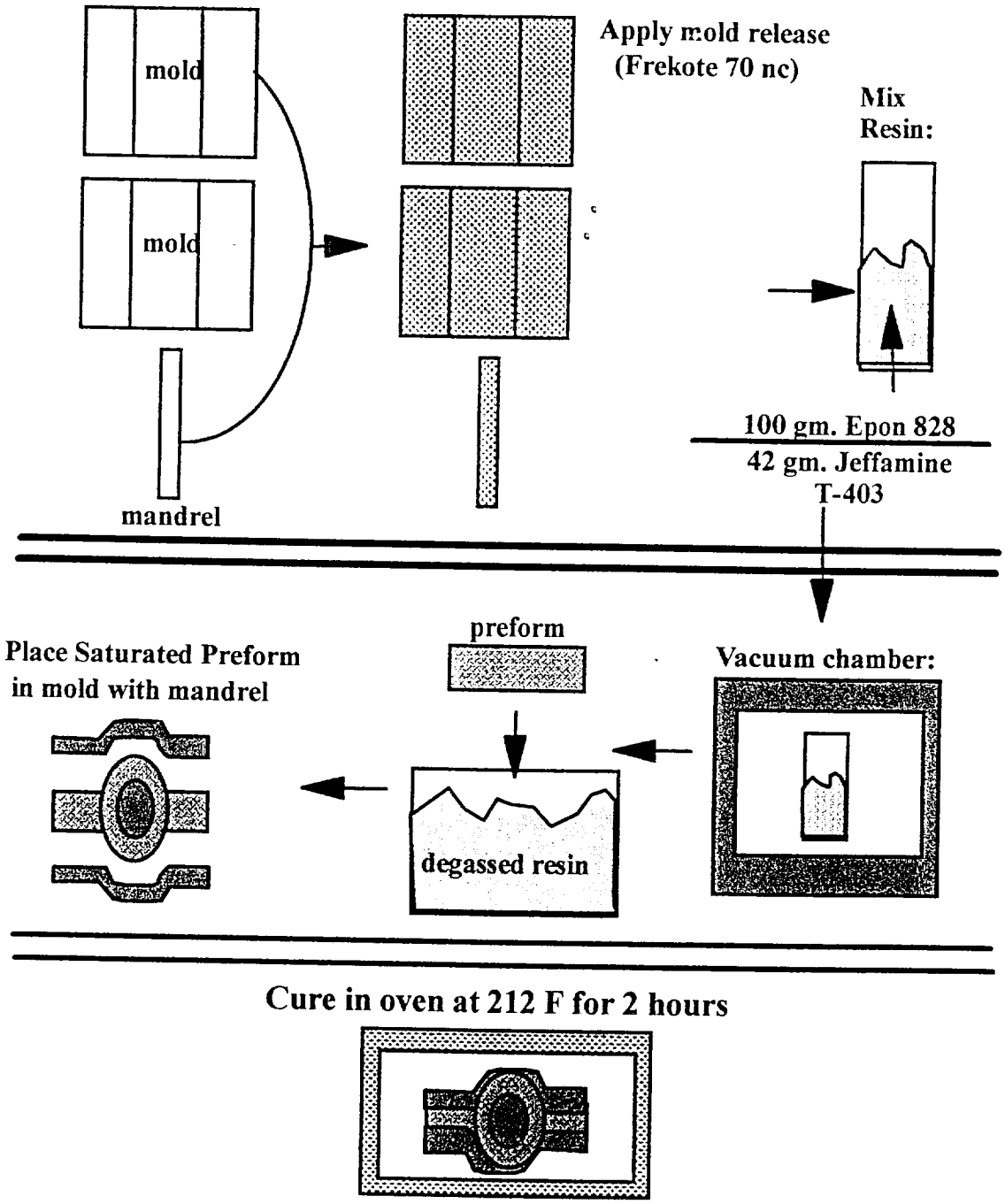

Figure 3.4- Infiltration of HMU preform

constructed of aluminum metal with an aluminum mandrel.

3.3 Infiltration of P100 HTS Preform

The infiltration of a copper/graphite material system is a very complex process because the two materials are incompatible and do not form a strong bond. In the early stages of this research, copper/graphite bars were produced and appeared to look fully infiltrated, but analysis of specimens proved that they were so weak that the mechanical bond could be broken by pulling on the bars by hand. Analysis of this system shows that graphite has little solubility in molten copper, copper will not form metal carbides, and the contact angle of liquid copper is so high that is beads up on the graphite surface(Weeks). The pressure required to force copper into a pore that does not wet is given as: $P = \left(\frac{2\gamma\cos(\theta)}{r}\right)$ where γ is the surface tension for the liquid copper, θ is the contact angle between liquid copper and the graphite fiber surface, r is the pore diameter and P is the pressure required to force the copper into the pore(Adamson). Analysis of this equation reveals that if the radius of the pore is small, a large amount of pressure is required. Joe Weeks stated ". . . 17 atmospheres of pressure is required for liquid copper to penetrate a pore with a radius of 1 micron". Since the graphite surface is very small, microns, it takes an enormous amount of pressure to cause the fibers to wet. In order to overcome the constraint of copper wetting the graphite tow, an intermediate interface consisting of a large amount of molybdenum carbide was used to coat the fibers. Using a method known as spontaneous liquid infiltration, TRA in Salt Lake City,

Utah was able to infiltrate the finned tube. TRA's coating process is proprietary and details pertaining to the process are unknown. However, figure 3.5 gives a schematic of the process. It is important to note that a good plasma coating will cause a preform to undergo an eleven percent weight gain after the preform has been through the coating process. Also during the plasma coating, the environment must be free of air and other contaminates, and it must be at constant temperature. If conditions are not satisfied, there will not be a continuous coating on the fibers surfaces and the un-coated fibers will not wet. The mold used in the process is shown in figures 3.6- 3.9. This mold was fabricated at TRA. The specimen dimensions were determined by considering a number of preforms and experiments with the epoxy component. All dimensions are interdependent and a change in one constitutes a changes in the others.

Based on casual observations the finned tube appeared to be fully infiltrated. However, after a section was cut and polished, the fiber coating did not penetrate through the entire surface resulting from a disconnection of the power source of the plasma machine during the plasma coating stage. This resulted in a break in the continuity of the fiber coating causing the fiber and copper not to bond completely throughout the component. Figures 3.10 - 3.12 show this discontinuity. Figure 3.11, the photo of the inner wall of the partially infiltrated tube, best represents this defect. Notice how there is a section of infiltrated copper right above unifiltrated fibers. This suggest that if the continuity of the fiber coating had not been interrupted, the tube would be infiltrated throughout the preform.

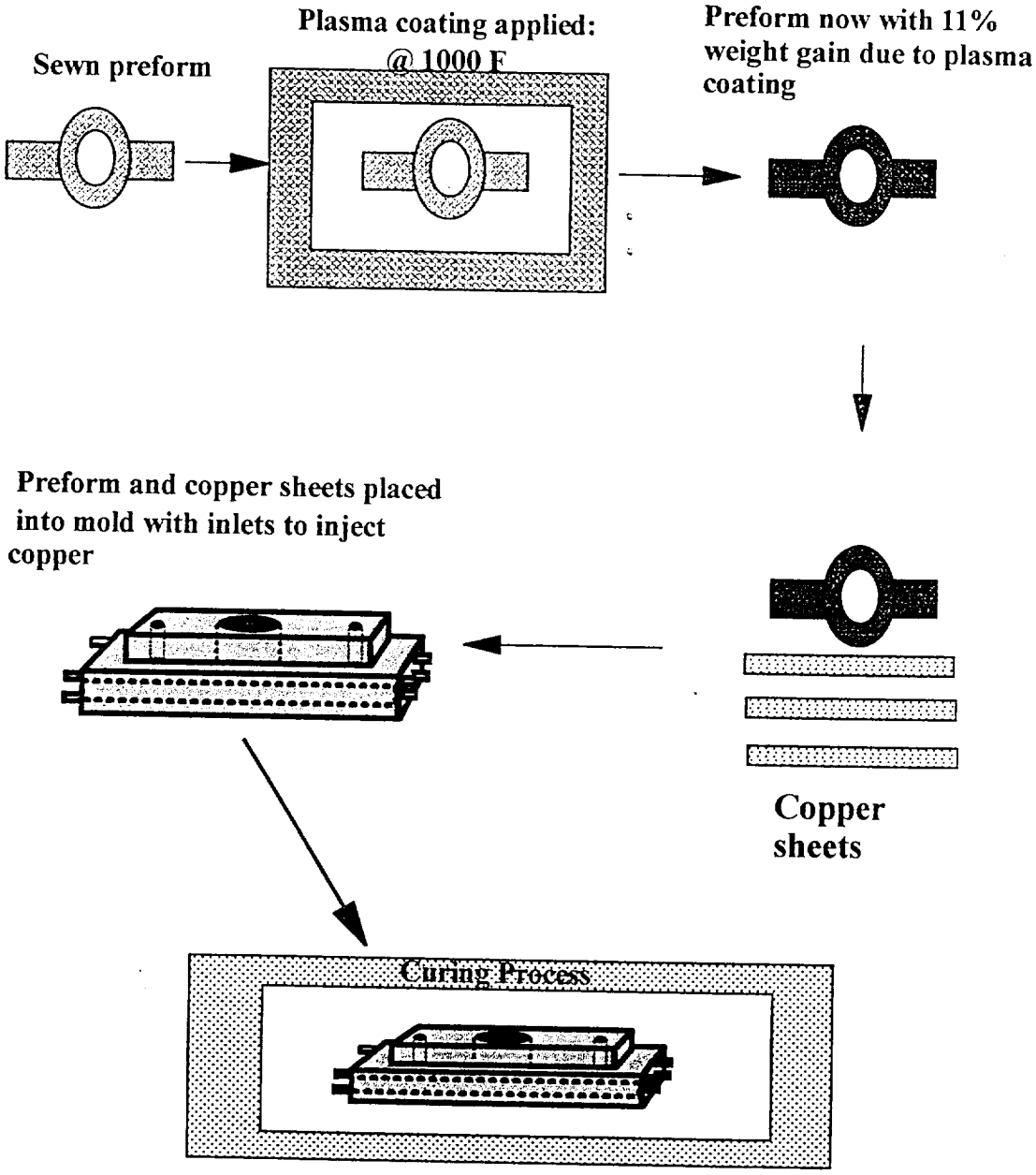

Figure 3.5 - Infiltration of P100 HTS preform

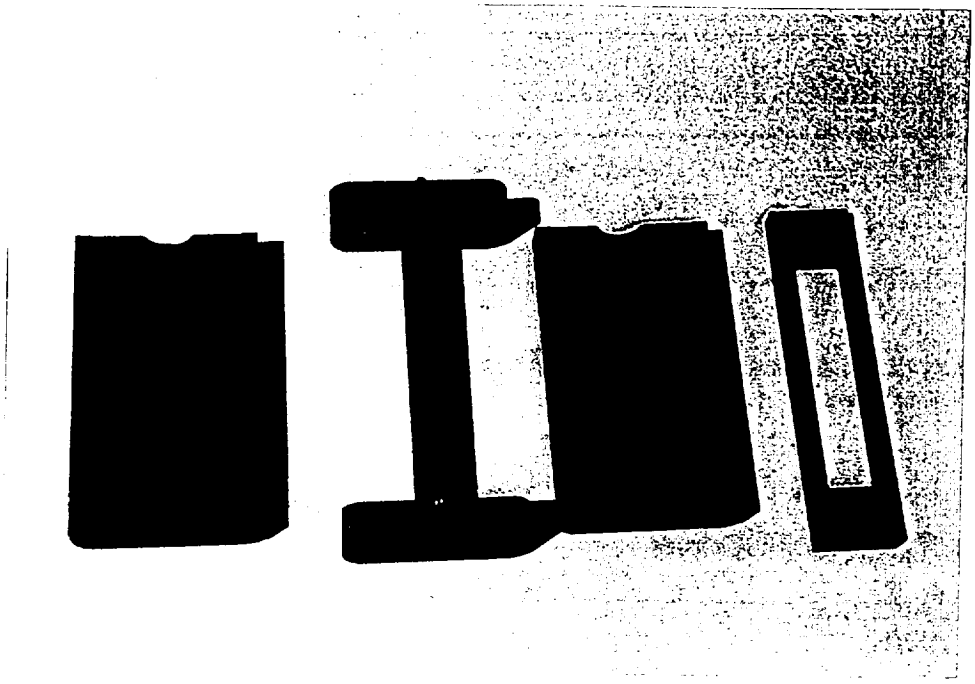

Figure 3.6 -Photo of disassembled mold.

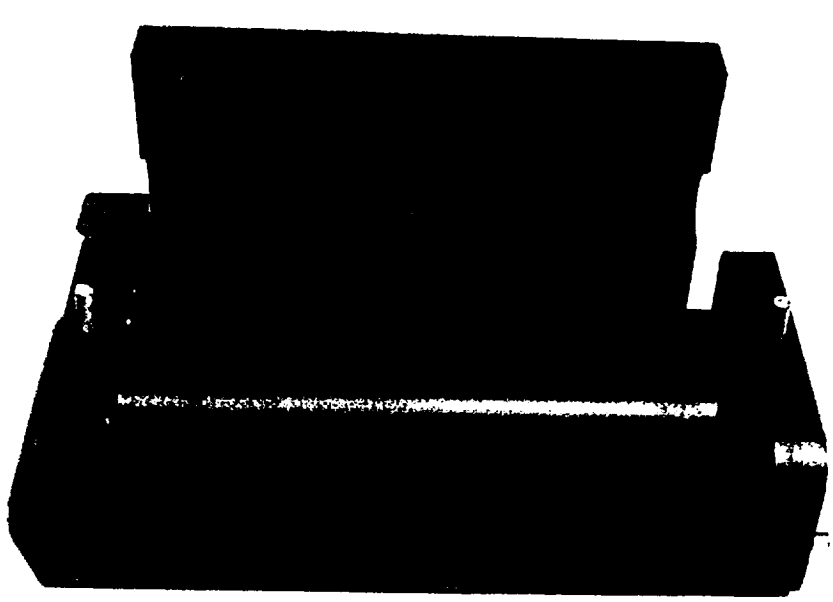

Figure 3.7 -Photo of assembling of mold .

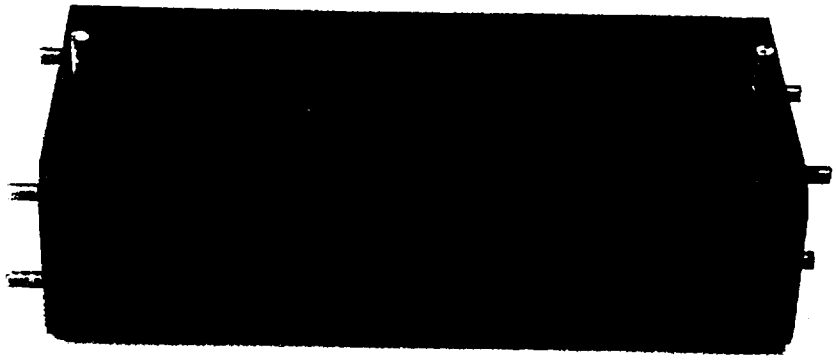

Figure 3.8 -Photo of assembling of mold.

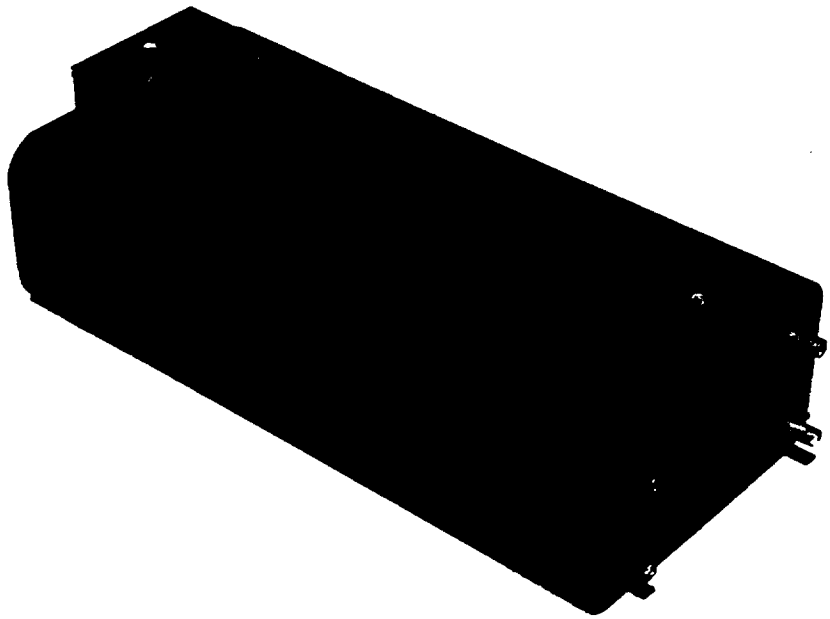

Figure 3.9 -Finished mold assembly.

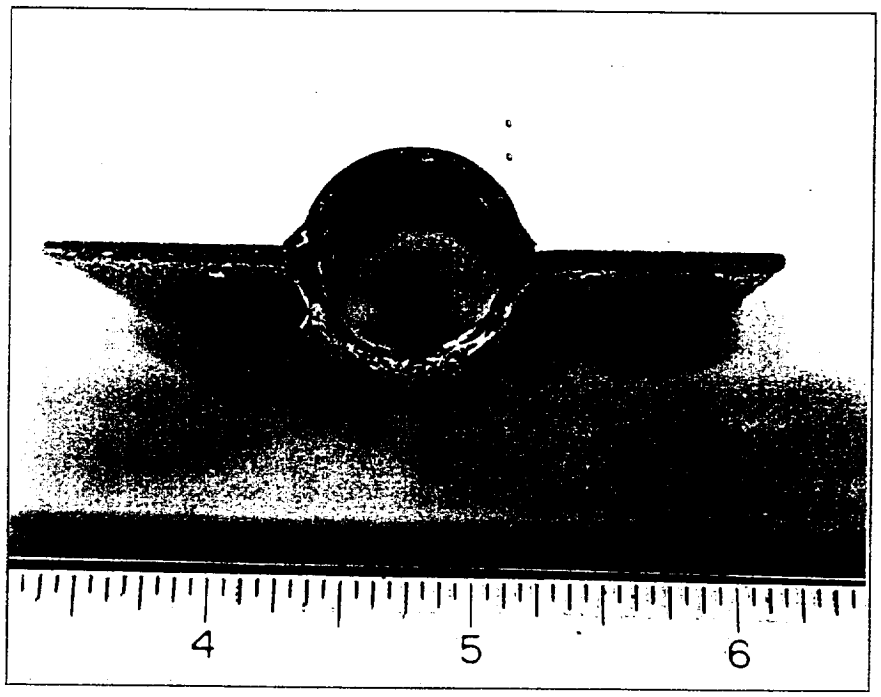

Figure 3.10 -Cross-section of first finned tube.

**** Notice that around the tube and fin joints there is uninfiltrated graphite****

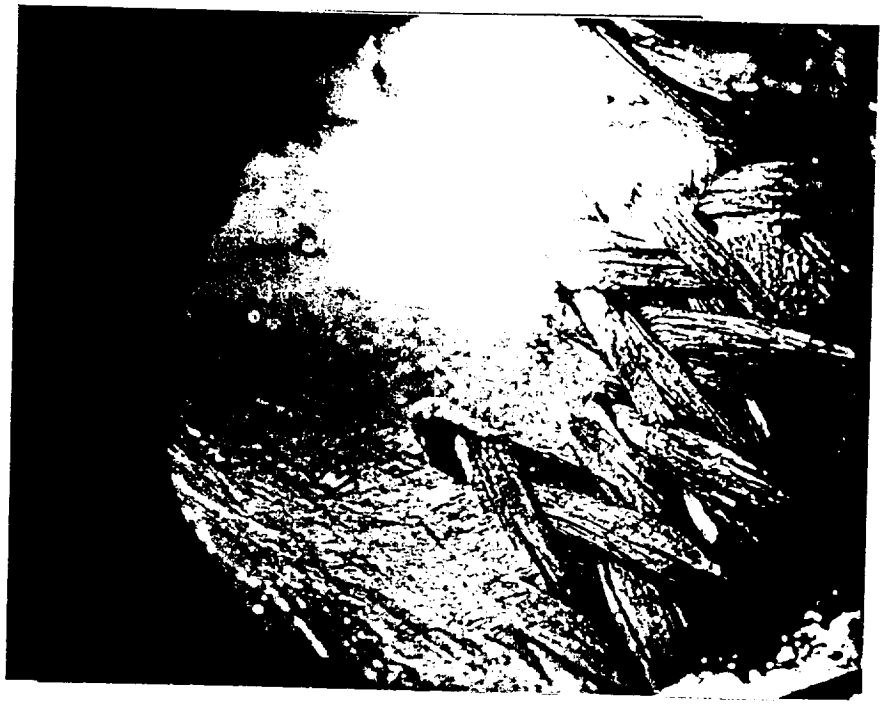

Figure 3.11 -Photo of first finned tube inner surface.

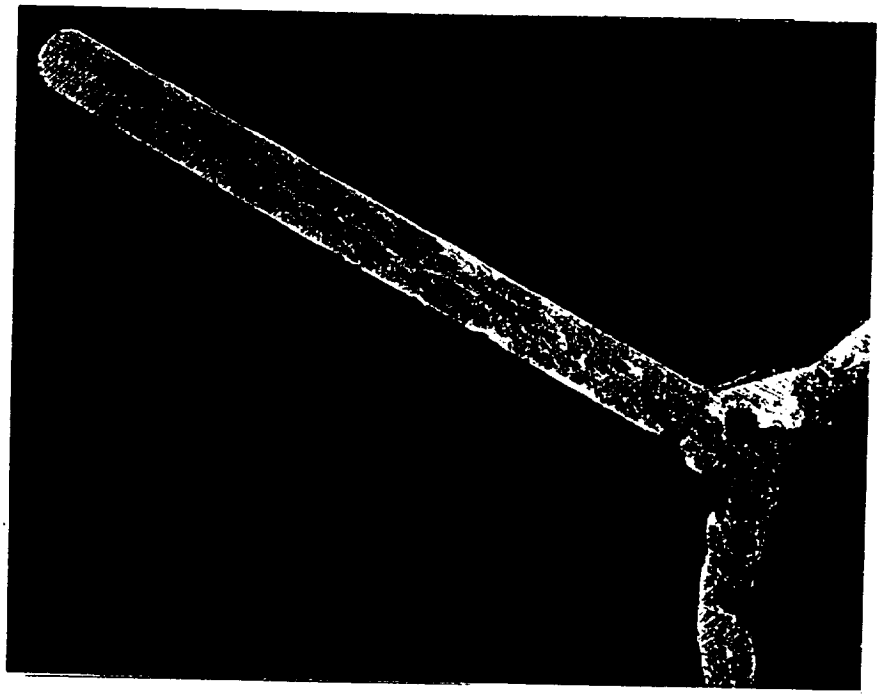

Figure 3.12 -Photo of fin and joint of first finned tube

Other photos show the un-wet fibers on the inside of the tube and at joints of the tube. The power interruption only permitted a six percent weight gain as opposed to the eleven percent needed to insure a good component.

The second attempt to coat the fibers produced a successful intermediary bond between the fibers and matrix, proving that the proof-of-concept finned tube graphite preform can be infiltrated with OFHC copper. Figures 3.13 - 3.21 show both the discontinuous and continuous components. Figure 3.17 was damaged when separating the component from the mold. Note that figure 3.21 is a photo of the fully infiltrated preform. It appears on the surface to have unwet fibers, but this is only a reflection of the copper grains on the fiber surfaces.

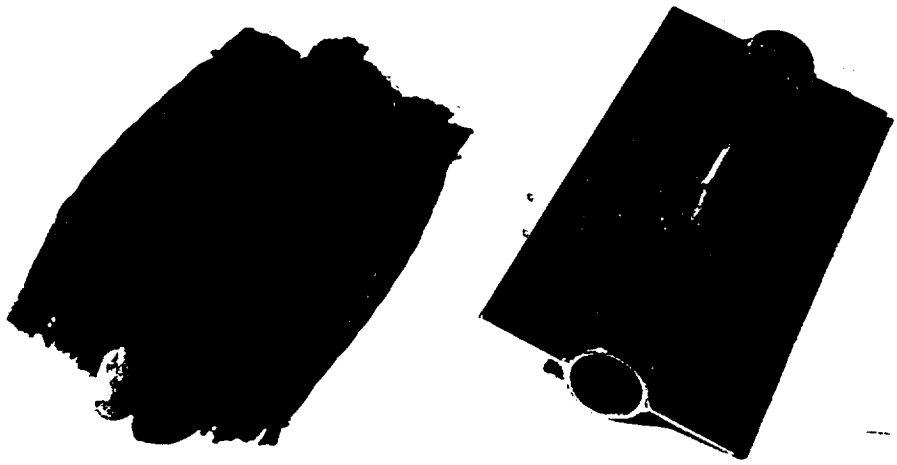

Figure 3.13 - Photo of finished component with stabilized preform

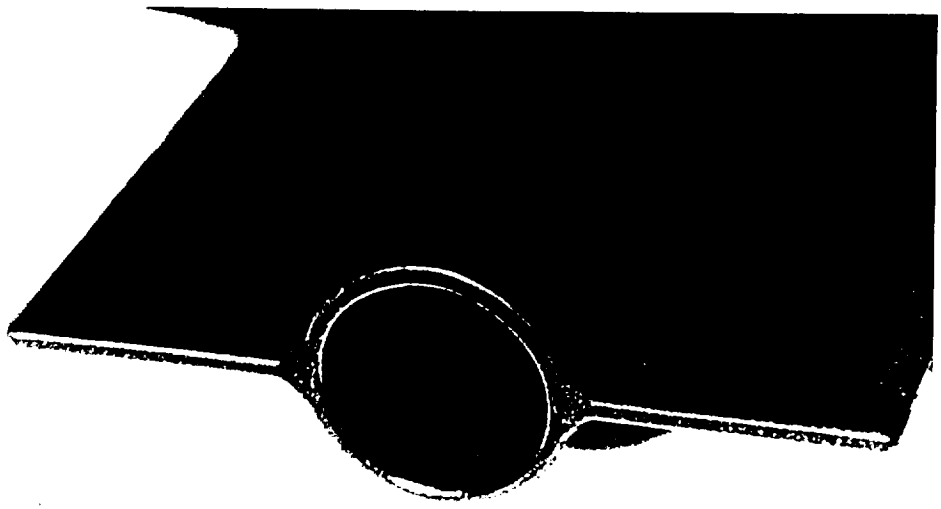

Figure 3.14 - Photo of end of first finned tube

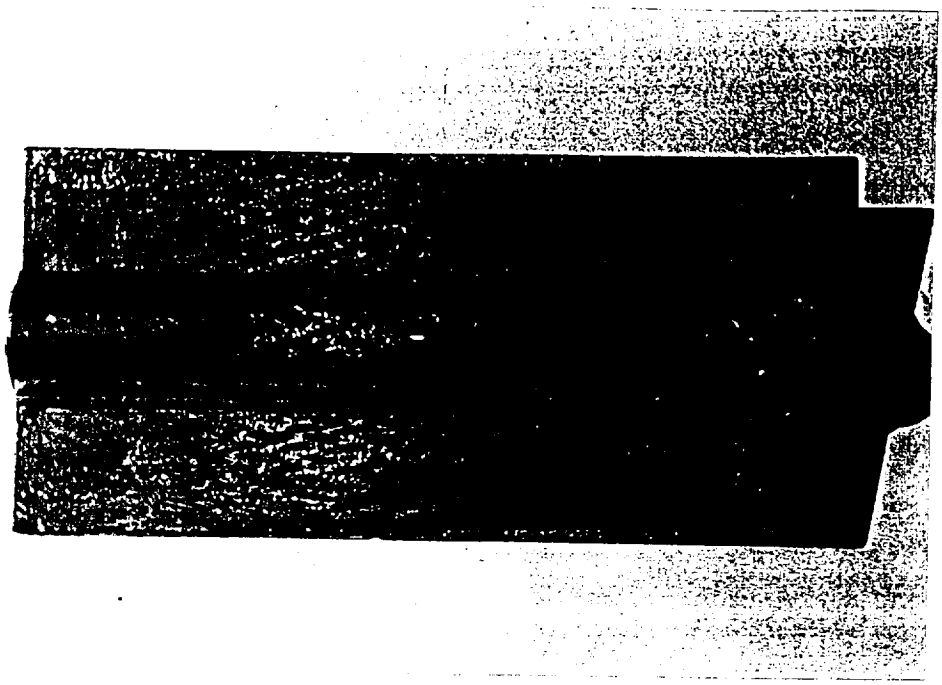

Figure 3.15 - Photo of Back of first finned tube. Notice sections that are not infiltrated.

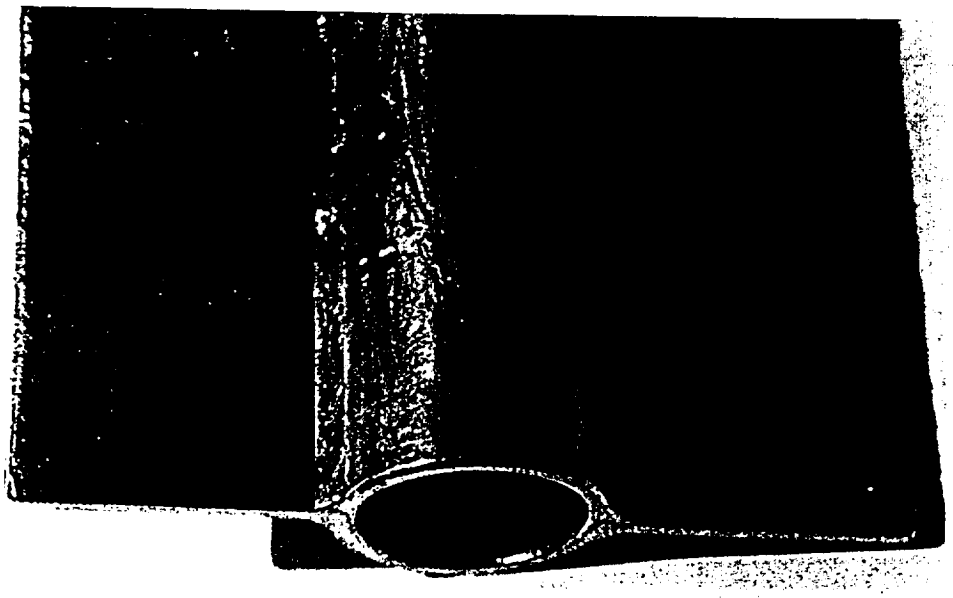

Figure 3.16 - Photo of good section of first finned tube. Notice the copper grains.

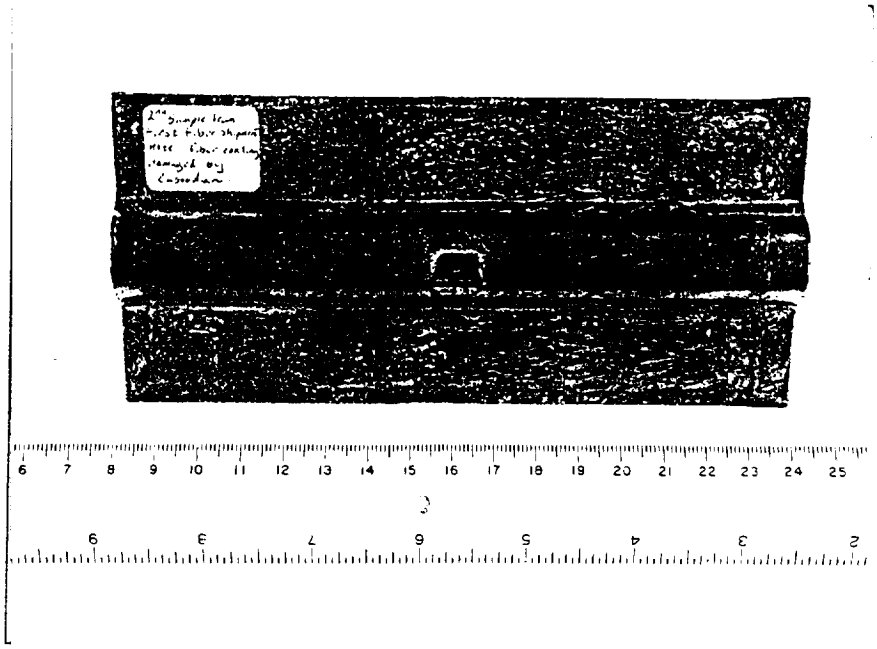

Figure 3.17 - Photo of second specimens. Note that there is still a uninfiltrated section because the plasma coating was applied at the same time of the first finned tube. This specimen was re-entered into the coating process, and results are same as first finned tube. Proving importance of coating the fibers successfully on first attempt.

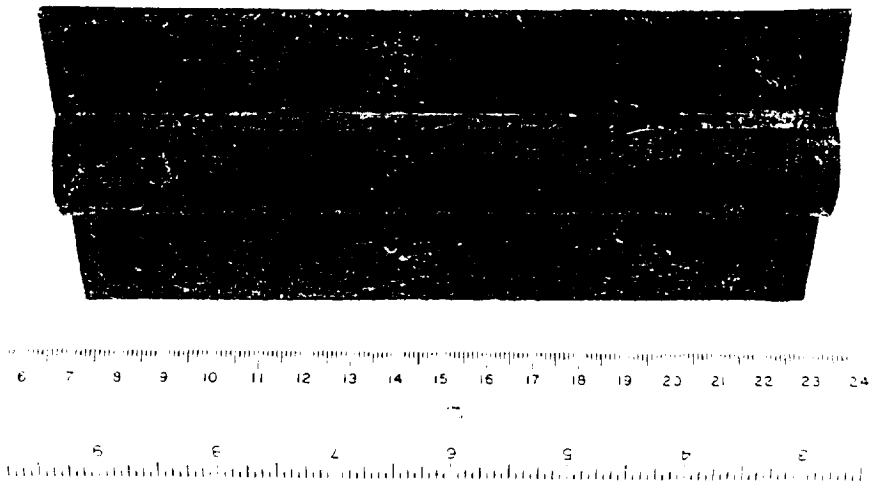

Figure 3.18 - Photo of the back of above tube.

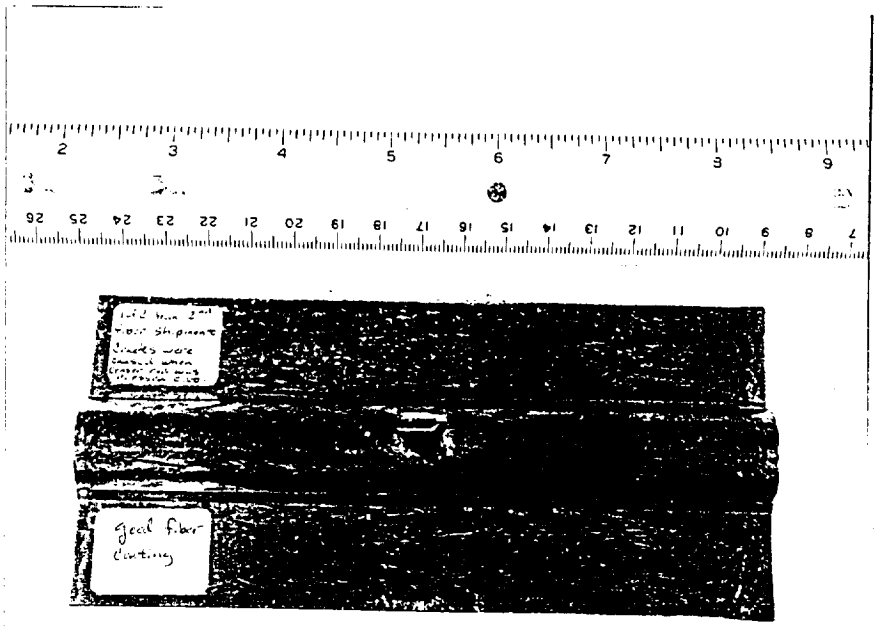

Figure 3.19 - This finned tube was damaged when the mandrel was pushed out, causing cracks.

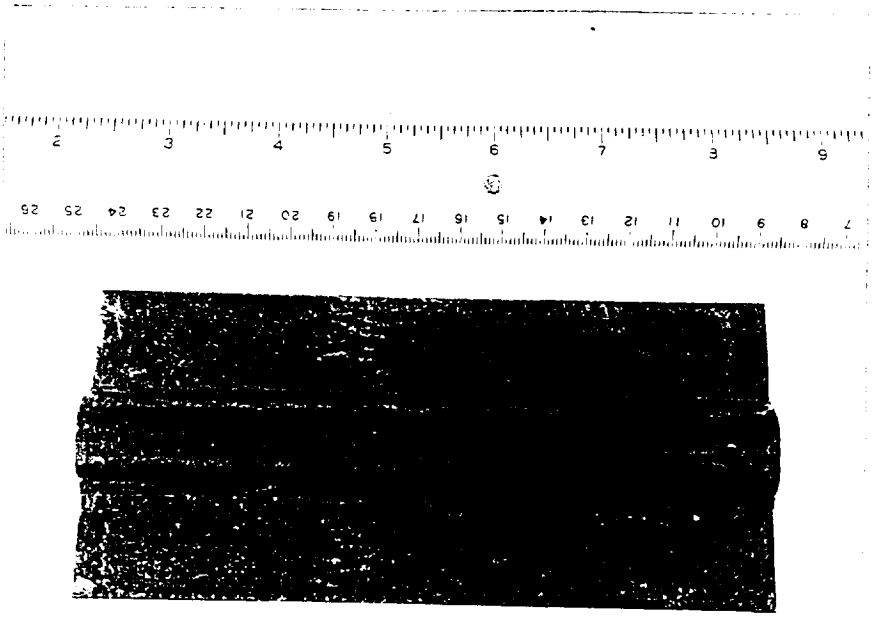

Figure 3.20 - Photo back of above tube. Notice that overall quality of this side is better than the other two attempts.

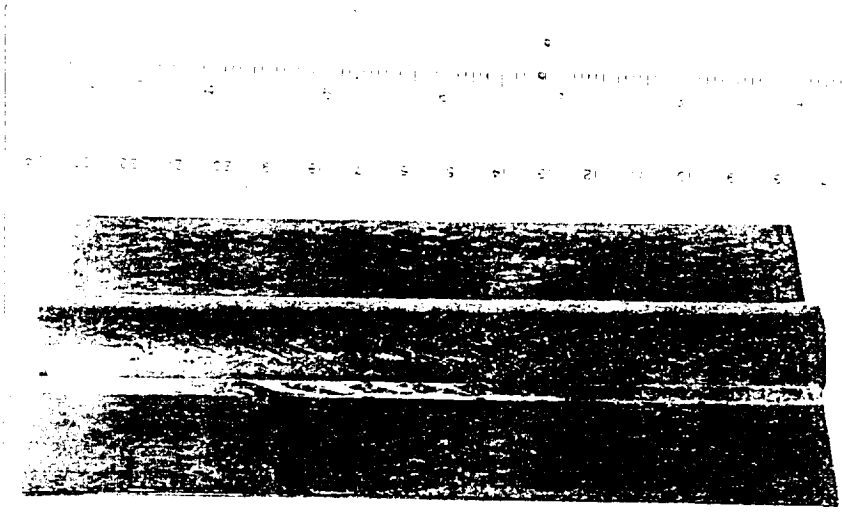

Figure 3.21 - Photo of the proof-of-concept finned tube. The copper grains can be seen throughout the entire specimen. This tube has a continuous fiber coating confirming the validity of the fabrication process for the finned tube.

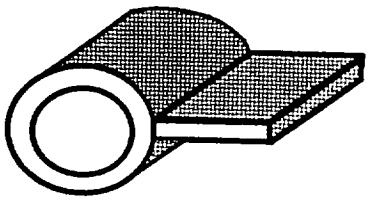

a)1 fin
1 tube

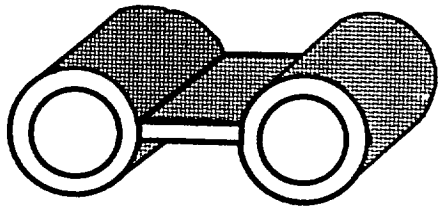

b) 1 fin
2 tubes

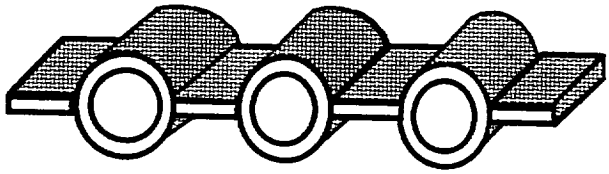

c) 4 fins
3 tubes

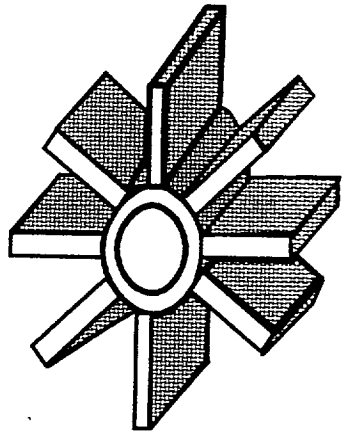

d) 7 fins
1 tube

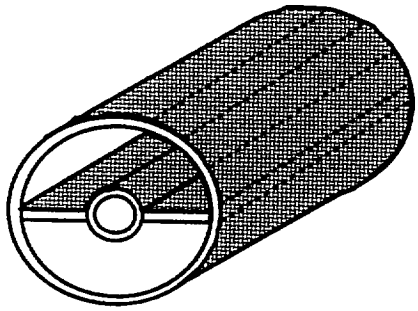

e) 2 fins and 1 tube surrounded by 1 tube

Figure 4.1 - Variety of possible braided finned configurations

These axials will not move throughout the preform and will be surrounded by existing braider carriers. If axials are used in a design, an alternative structural map would have to be provided in order to predict the components properties. Although axials were not used in this project, the carrier has the capability to produce a component with axials. The axial carriers can be seen in figures 2.7- 2.10. The axial carriers will be the spaces with empty carriers between each radial column.

4.2 Mechanical Implications

Using the knowledge of the braiding process, specific mechanical properties can be implemented into the design of components. In order to control the stiffness or toughness of a component, different volume fraction ratios should be used. Thus, depending on the function of the component, the structural properties can be tailored for suitability for the situation. If longitudinal reinforcement is needed, axials can be used in the braiding process. In either case, the mechanical properties have to be varied with the geometry in order to obtain the overall desired properties.

4.3 Hybridization and Thermal Implications

Based on the analysis of the geometry of a braided finned tube, there are certain positions on the carriers that move in a less rigorous pattern. Since the positions can be linked to the braider groups on the carrier, a logical deduction could be to place different materials in various braiding paths. This arrangement would introduce a wide variety

of configurations. For example, in the beginning of the research, K 1100-x fibers were preferred because of their superior conduction and structural properties, but these fibers were impossible to braid. By introducing the K1100-x fibers as axials with P100 HTS fibers braiding around them in the fin tube, the structural rigidity and thermal conduction properties would increase. Therefore, if an improvement in the properties of the P100 HTS/ copper matrix finned tube is needed, hybrid axials could be a viable solution.

The use of hybridization can also be used to direct the thermal conduction of a component if high conductivity and low conductivity fibers are used simultaneously. An example would be to use low conductivity fibers to braid the tube and high conductivity fibers to braid the fins. In this case, most of the thermal conduction would take place in the fins, proving that hybridization is a valid consideration in the designs of components. Thermal properties could also be increased by adding K-1100 X axials to the P100 preform. Although there would be some heat transfer between different tows, the overall thermal properties would improve.

The use of hybridized braided components could be used to aid heat dissipation in gun and tank barrels if tough fibers are used in the barrels to absorb the hoop stresses and high conductivity fibers are used in fins to dissipate the heat. Other possibilities of a 3-D braided fin tube could range from refrigerant tubes to computer circuit board technology.

Although hybridization of these braided components offers several advantages, there are some limiting factors that need to be discussed. When two different fibers are used,

the fibers need to have compatible thermal coefficients of thermal expansion (CTE). Failure to have similar coefficients of expansions will result in internal stresses that may nullify the advantages that were gained by hybridizing, especially at joining sections. The difference in the CTE's may also cause thermal racheting in the heat flow. Internal stresses can also be introduced between stiff and tough fibers. Therefore, it is important to understand the materials and their compatibility before hybridization is attempted.

CHAPTER FIVE

CONCLUSIONS

5.1 Conclusions

The original proof-of-concept finned tube was fabricated and appeared to look very good, but the infiltration did not penetrate through the entire preform in the first component due to discontinuity of the plasma coating. However, when the plasma coating was tried the second time it produced a continuous coating which resulted in a good component. Based on the facts presented in this thesis, other configurations can be conformed to the design of components. This research should be used as a guideline for braiding and infiltration of integral high conductivity complex components.

5.2 Future Work

Exploration should be attempted on configurations using highly conductivity hybridized materials. This will open the door to interesting light weight, highly conductive, robust, high strength materials that can operate effectively at high temperatures. Baseline uniaxial bars made of the same OFHC copper and high conductivity graphite material system should be fabricated in order to aid in the modeling of the complex braid structure.

REFERENCES

Adamson, A. Physical Chemistry of Surfaces. 3rd Edition. John Wiley and Sons, (1976).

Jones, Robert M. Mechanics of Composite Materials. New York; Hemispere, 1975.

Taya, Minoru and Richard J. Arsenault. Metal Matrix Composites. Thermomechanical Behavior. New York: Pergamon, 1989.

Li, Wei and Aly El Shiekh. "The Effect of Processes and Processing Parameters on 3-D Braided Preforms For Composites." SAMPE Quarterly 19.4 (1988) : 22-28.

Hammad, M., El-Messery and A. El Shiekh. "Structural Mechanics of 3-D Braided Preforms for Composites, Part 4 : The 4-Step Tubular Braiding." 36th International SAMPE Symposium. April 15-18, 1991. 114-129.

Bednarcyk, Brett A. and Mared-Jerzy Pindera. "Micromechanical Modeling of The Thermal Expansion of Graphite/Copper Composites with Nonuniform Microstructure." NASA Contractor Report 195368. August 1994.

Lee, Bruce Edward. "Three Dimensional Braided Graphite Preforms with Copper Matrix Composites." Diss. North Carolina Agricultural and Technical State University, 1996.

Weeks, Joe. "Copper/Graphite Composite Fabrication Background." Unpublished essay, 1996.

---. Telephone interviews. June-July 1996.

Reid, Rhona. Personal interviews. 1994-96.

---. Telephone interviews. 1994-96.

* Most of the information contained in this thesis was obtained by observation and experimentation at the Mars Mission NASA Lab at North Carolina State University.

APPENDIX

Detailed Fiber Specifications

The P100 HTS fibers used in this research had a tow size of 2K (2000 fibers per tow). In order to achieve the desired geometry and inner diameter specifications, the tows were taped together to form 6K tows. For a more detailed fiber property description, please see the fiber certification below.

Fiber Certification as obtained by Amoco Performance Products, Inc.

3 spools of (0.50 #) Thornel carbon fiber with grade P-100 HTS and 2K tows with AP-200 sizing were Cross Wound and had shear treatment. APPI Reference # 12030071. These fibers had the following average properties:

Lot S940107

Trace HSL-813

Tensile Strength 593 ksi	Tensile Modulus 104.3 msi
Density 2.163 gm/cc	Yield 0.319 gm/m
Torsional Shear Strength 8.25 ksi	Twist NO